

Primal-Dual Interior-Point Method for Thermodynamic Gas-Particle Partitioning

Alexandre Caboussat ^{*†}

Abstract

A mathematical model for the computation of the phase equilibrium and gas-particle partitioning in atmospheric organic aerosols is presented. The thermodynamic equilibrium is determined by the global minimum of the Gibbs free energy under equality and inequality constraints for a system that involves one gas phase and many liquid phases. A primal-dual interior-point algorithm is presented for the efficient solution of the phase equilibrium problem and the determination of the active constraints. The first order optimality conditions are solved with a Newton iteration. Sequential quadratic programming techniques are incorporated to decouple the different scales of the problem. Decomposition methods that control the inertia of the matrices arising in the resolution of the Newton system are proposed. A least-squares initialization of the algorithm is proposed to favor the convergence to a global minimum of the Gibbs free energy. Numerical results show the efficiency of the approach for the prediction of gas-liquid-liquid equilibrium for atmospheric organic aerosol particles.

1 Introduction

The prediction of liquid-liquid equilibria and gas-particle partitioning for organic aerosol particles is an important problem in the determination of the microphysics of atmospheric aerosols [3, 23, 31, 33, 34].

The phase equilibrium of a gas-particle system is characterized by the global minimum of the Gibbs free energy of the system [22, 24, 28, 29]. It is equivalent to the stationary solution of a transient problem when gas and liquid phases exchange mass [4]. The minimization of Gibbs free energy constrained by mass balance is a standard approach in order to solve phase equilibrium problems. Minimization methods for the particle thermodynamics have been presented for instance in [27, 40, 48], while extensions to the gas-particle problem have been addressed in [23, 30, 39]. They either rely on a direct minimization of the Gibbs free energy or on the minimization of the tangent-plane distance function (flash calculations) [25, 30, 48]. However, such methods either are too computationally intensive or not accurate enough, which makes their use in three-dimensional air quality models infeasible.

We address here the problem of the determination of the thermodynamic equilibrium for one single organic aerosol particle. Chemical problems usually induce large differences of scales in

^{*}Affiliation: University of Houston, Department of Mathematics, 4800 Calhoun Rd, Houston, Texas 77204 - 3008, USA. Email: caboussat@math.uh.edu

[†]Partially supported by University of Houston New Faculty Grant I094138 and U.S. Environmental Protection Agency Grant X-83234201

the gas and liquid concentrations and large differences of reaction speeds. The gas concentrations in the atmosphere are known to be much smaller than the concentrations in the aerosol particle, leading to an ill-conditioned problem [24]. Therefore decomposition techniques have to be designed for an efficient direct computation of the minimum of energy [12, 20, 21].

A primal-dual interior-point algorithm is used here for the efficient solution of the equilibrium problem. Sequential quadratic programming techniques are incorporated in order to decouple the gas phase from the particle phases in the resolution of the Karush-Kuhn-Tucker (KKT) system. To encourage the convergence to a global minimum, an adapted initialization of the algorithm is presented, which fully uses the geometric and homogeneity properties of the Gibbs free energy function.

The algorithm applies at each step a Newton method to the Karush-Kuhn-Tucker (KKT) system of equations, perturbed by an interior-point parameter term, to find the next primal-dual approximation of the solution. Convexification methods are implemented when needed to keep the Hessian matrix of the objective function positive definite and help the convergence to a global minimum. Sequential quadratic programming techniques decouple the Newton system into two sub-problems coupled through an unconstrained convex minimization problem. They allow to incorporate the numerical linear algebra techniques previously developed in [2] for the particle phase. An active sets procedure is incorporated for the accurate detection of the *active* (or *non-empty*) phases at equilibrium in the particle.

Global and local convergence properties of primal-dual interior-point methods is a difficult issue in nonlinear programming. Even in some simple cases, convergence to a feasible solution cannot be guaranteed, as illustrated in [44]. The importance of the merit functions has been emphasized in [17, 41], without being able to conclude to the global convergence of the method in all cases. One well-known problem inducing the lack of convergence is the so-called *jamming* problem [6, 8, 44]. This issue usually requires the modification of the search direction that satisfy some linearization of the constraints in the KKT conditions, or the modification of the KKT system itself with some penalty function.

Global (and local) convergence studies for primal-dual interior-point methods have been presented *e.g.* in [9, 14, 18, 45, 46, 49]. Judicious merit functions are suggested [18], or trust region or filter methods are advocated [9, 49]. Second order corrections of the solution of the KKT system ensure local convergence [45, 46] in some cases. Convergence can also be encouraged with an adequate starting point of the algorithm, as for instance in warmstarting techniques [7, 21].

In this article, we suggest a primal-dual interior-point method. Although, no formal proof of global convergence can be given, the suggested algorithm implicitly incorporates several of the above issues. The problem of interest is a regular, small, perturbation of the liquid-liquid equilibrium problem addressed in [2], that admits some convergence results [36]. The method introduced in [2] allows a judicious initialization of the interior-point method for the gas-particle problem incorporating some kind of warmstarting effects. The active sets method provides a modification (by truncation) of the search direction obtained by the solution of the KKT system that avoids the jamming problem emphasized in [6, 8, 44]. Numerical results show the convergence of the algorithm to a feasible solution, that is close to the global optimum of the problem presented in [2]. Under the chemical assumption that the gas concentrations are small with respect to the particle concentrations, this feasible solution is a good candidate for a global

optimum.

The structure of this paper is the following. In Section 2, the mathematical modeling of the gas-particle partitioning problem for organic aerosols and the corresponding optimization framework are presented. In Section 3, a sequential quadratic programming approach is coupled to the primal-dual interior-point method, and the linear algebra and resolution methods are discussed. The initialization procedure is discussed in Section 4. Numerical results are finally presented in Section 5 to illustrate the efficiency of the method. Finally, since many general purpose NLP solvers exist in the literature (*e.g.* IPOPT [43, 47], Knitro [10, 11] or LOQO [8, 42]), the results obtained with the proposed method are compared with those obtained with the solver IPOPT.

2 Modeling of the Phase Equilibrium Problem

The phase equilibrium for organic aerosols with gas and liquid phases is given by the global minimum of the Gibbs free energy of the system. Let \mathbb{R}_+ denote the set of non-negative real numbers and \mathbb{R}_{++} the set of strictly positive real numbers. Consider a chemical system composed of $n + 1$ substances at a specified temperature and pressure. For a given feed-vector $\bar{\mathbf{b}} \in \mathbb{R}_{++}^{n+1}$, the thermodynamic equilibrium of the system is given by the solution of the constrained minimization problem

$$\min G(P, y_\alpha, \mathbf{x}_\alpha, \mathbf{n}_g) = \sum_{\alpha=1}^P y_\alpha g(\mathbf{x}_\alpha) + \mathbf{n}_g^T (\boldsymbol{\mu}_g(\mathbf{n}_g) - \mathbf{e}_{n+1}), \quad (1)$$

$$\text{s. t.} \quad \sum_{\alpha=1}^P y_\alpha \mathbf{x}_\alpha + \mathbf{n}_g = \bar{\mathbf{b}}, \quad (2)$$

$$y_\alpha \geq 0, \quad \alpha = 1, \dots, P, \quad (3)$$

$$\mathbf{x}_\alpha > 0, \quad \mathbf{e}_{n+1}^T \mathbf{x}_\alpha - 1 = 0, \quad \alpha = 1, \dots, P, \quad (4)$$

$$\mathbf{n}_g > 0, \quad (5)$$

where P is the number of liquid phases inside the particle, $y_\alpha \in \mathbb{R}_+$ is the number of moles in each liquid phase α , $\mathbf{x}_\alpha \in \mathbb{R}_{++}^{n+1}$ is the mole-fraction concentration vector in phase α , for $\alpha = 1, \dots, P$, and $\mathbf{n}_g \in \mathbb{R}_{++}^{n+1}$ is the concentration vector in the gas phase. Here \mathbf{e}_k denotes the vector in \mathbb{R}^k , $k \in \mathbb{N}$, such that all components are equal to 1. The first term in the energy (1) corresponds to the contribution to the total energy provided by the liquid phases, while the second term is the contribution from the gas phase. The equality constraints (2) correspond to the conservation of mass. Relationship (5) implies that the gas phase always exists with positive concentrations and only the liquid phases can be emptied/filled (activated/deactivated) (3). The number of liquid phases P at equilibrium is *a priori* unknown. In order to write the problem (1)-(5), we make the following (chemical) assumptions [38]:

(H1) All the phases in the system belong to a same phase class so that the Gibbs free energy function g is the same for all liquid phases.

(H2) All substances can partition into all phases and no reactions are possible between them.

(H3) For all $\alpha = 1, \dots, P$, if there exists $j \in \{1, \dots, n+1\}$ such that $\mathbf{x}_{\alpha,j} > 0$, then $\mathbf{x}_\alpha > 0$.

Assumptions (H1)(H2) are chemical assumptions from the model and the chemical species considered. Assumption (H3) is more restrictive, but common in atmospheric chemistry models. It allows the chemical model for the Gibbs free energy function g to be well-defined. The molar Gibbs free energy g satisfies $g \in C(\mathbb{R}_+^{n+1}) \cap C^\infty(\mathbb{R}_{++}^n)$ and $\lim_{x_i \rightarrow 0} \frac{\partial g}{\partial x_i} = -\infty$, for all $i = 1, \dots, n+1$, that is, the values of g approach finite limits as any given mole fraction tends to zero, and these limiting values are approached with negatively infinite slope. For organic-containing particles, the energy function is given by the UNIFAC model [19]. The chemical potential $\boldsymbol{\mu}_g$ is explicitly given by $\boldsymbol{\mu}_g(\mathbf{n}_g) = \ln\left(\mathbf{n}_g \frac{RT}{p_{\text{vapor}}}\right) = \ln(\mathbf{n}_g) + \ln(RT) - \ln(p_{\text{vapor}})$, where p_{vapor} is the vector of vapor pressures corresponding to the chemical species [35], $R = 8.20575 \cdot 10^{-5}$ [m³ atm mol⁻¹K⁻¹] is the universal gas constant and T is the ambient temperature (usually $T = 298.15$ [K]).

Because of the *Gibbs-Duhem* relation [13], the Hessian of the objective function g is only positive semi-definite and the sufficient second order optimality conditions corresponding to (1)-(5) are not necessarily satisfied. In order to eliminate the zero eigenvalues of the Hessian and obtain a well-posed optimization problem, we project (1)-(5) on the normalization constraints (4). Let $\mathbf{z} = \mathcal{P}\mathbf{x}$ denote the projection of $\mathbf{x} \in \mathbb{R}^{n+1}$ such that $\mathbf{e}_{n+1}^T \mathbf{x} = 1$ onto \mathbb{R}^n defined by $\mathcal{P}(x_1, \dots, x_n, x_{n+1}) = (x_1, \dots, x_n)$. Let us denote $\mathbf{z}_\alpha = \mathcal{P}\mathbf{x}_\alpha$, $\mathbf{b} = \mathcal{P}\bar{\mathbf{b}}$ the reduced mole-fraction and feed vectors and $\tilde{\mathbf{b}} = \mathbf{e}_{n+1}^T \bar{\mathbf{b}}$ the number of moles in the system. Let $\Delta_n = \{\mathbf{z} \in \mathbb{R}^n : \mathbf{e}_n^T \mathbf{z} \leq 1, \mathbf{z} \geq 0\}$ be the unit simplex and $\text{int}\Delta_n$ its interior. Let f be the energy function defined by $f(\mathbf{z}) = g(\mathbf{x})$, where $\mathbf{x} = (\mathbf{z}, 1 - \mathbf{e}_n^T \mathbf{z})^T$. Then, f is continuous on Δ_n , C^∞ on $\text{int}\Delta_n$, and has a subdifferential $\partial f(\mathbf{z}) = \emptyset$ for $\mathbf{z} \in \partial\Delta_n$ [5]. We consider the set of functions f (see [2]) such that:

(H4) For each vertex of Δ_n , there exists a neighborhood \mathcal{N} such that the function f is convex on $\Delta_n \cap \mathcal{N}$, *i.e.* $\nabla^2 f(\mathbf{d}) > 0$, for all $\mathbf{d} \in \Delta_n \cap \mathcal{N}$.

Assumption (H4) is of a chemical nature, since pure solutions (*i.e.* solutions with only one chemical component) are thermodynamically stable. Problem (1)-(5) is equivalent to

$$\begin{aligned}
\min \quad & G = \sum_{\alpha=1}^P y_\alpha f(\mathbf{z}_\alpha) + \mathbf{n}_g^T (\boldsymbol{\mu}_g(\mathbf{n}_g) - \mathbf{e}_{n+1}), \\
\text{s. t.} \quad & \sum_{\alpha=1}^P y_\alpha \mathbf{z}_\alpha + \mathcal{P}\mathbf{n}_g = \mathbf{b}, \\
& \sum_{\alpha=1}^P y_\alpha + \mathbf{e}_{n+1}^T \mathbf{n}_g = \mathbf{e}_{n+1}^T \bar{\mathbf{b}} = \tilde{\mathbf{b}}, \\
& y_\alpha \geq 0, \quad \alpha = 1, \dots, P, \\
& \mathbf{z}_\alpha \in \text{int}\Delta_n, \quad \alpha = 1, \dots, P, \\
& \mathbf{n}_g > 0.
\end{aligned} \tag{6}$$

This problem is related to the determination of the convex envelope of the function f , see [1]. Indeed, consider the case where \mathbf{n}_g is given and let $\mathbf{d} := (\mathbf{e}_{n+1}^T (\mathbf{b} - \mathbf{n}_g))^{-1} (\mathbf{b} - \mathcal{P}\mathbf{n}_g) \in \Delta_n$. Problem (6) corresponds, as an application of Carathéodory's theorem, to the determination of the value of the convex hull $\text{conv}f(\mathbf{d})$ of the given energy f at the point \mathbf{d} (where the convex

hull is defined as the largest convex real-valued function majored by f on Δ_n). The hyperplane defined by the set of points $\{(\mathbf{z}_1, f(\mathbf{z}_1)), \dots, (\mathbf{z}_P, f(\mathbf{z}_P))\}$ is called *supporting tangent plane* of the non-convex function f . In other words, (6) corresponds to finding the set of contact points $\{\mathbf{z}_1, \dots, \mathbf{z}_P\}$ between the function f and the supporting tangent plane, together with the corresponding barycentric coordinates y_1, \dots, y_P of \mathbf{d} such that $\sum_{\alpha=1}^P y_\alpha \mathbf{z}_\alpha = \mathbf{d}$. For sufficiently smooth functions f (namely functions f in a residual set of $E = \{f \in C^\infty(\text{int}\Delta_n) : f \in C^0(\Delta_n), \partial f(\mathbf{z}) = \emptyset \text{ for } \mathbf{z} \in \partial\Delta_n\}$), the supporting tangent plane is unique and the decomposition of \mathbf{d} into a convex combination of (up to) $n + 1$ points $\{\mathbf{z}_1, \dots, \mathbf{z}_{n+1}\}$ is unique (see [36]).

The points \mathbf{z}_α belong to convex regions of the function f [1]. This remark has significant implications for the proposed algorithm, and in particular for the initialization of the variables \mathbf{z}_α in the convex regions of f . The goal of the algorithm is to compute the sequence of points \mathbf{z}_α that are the contact points between the function f and its supporting tangent plane, such that each point remains in a convex region of f and such that the convex combination $\sum_{\alpha=1}^P y_\alpha f(\mathbf{z}_\alpha)$ is minimized.

A more complete description of the geometrical structure of f and its convex envelope can be found in [1, 36]. The addition of the term $\mathbf{n}_g^T(\boldsymbol{\mu}_g(\mathbf{n}_g) - \mathbf{e}_{n+1})$ transforms the convex envelope. The geometric interpretation of the determination of the convex envelope of f that is valid when \mathbf{n}_g is given, is therefore obsolete. However these geometric properties can be extended for a suitable initialization of the algorithm proposed in this paper. Since, in atmospheric chemistry, $\mathbf{n}_g \ll \sum_{\alpha=1}^P y_\alpha \mathbf{z}_\alpha$, the insertion of the extra term can be considered as a perturbation of the convex envelope problem. The objective function G being convex in terms of the variable \mathbf{n}_g , the following result holds:

Theorem 1 *The problem (6) admits a unique global minimizer.*

Proof. The problem (6) can be written as

$$\begin{aligned} \min_{\mathbf{n}_g} \quad & G = \mathbf{n}_g^T(\boldsymbol{\mu}_g(\mathbf{n}_g) - \mathbf{e}_{n+1}) + \mathcal{H}(\mathbf{n}_g), \\ \text{s. t.} \quad & \mathbf{n}_g > 0. \end{aligned} \tag{7}$$

where $\mathcal{H}(\mathbf{n}_g)$ is the solution for given \mathbf{n}_g of the constrained optimization problem

$$\begin{aligned} \mathcal{H}(\mathbf{n}_g) = \min_{\mathbf{z}_\alpha, y_\alpha} \quad & \sum_{\alpha=1}^P y_\alpha f(\mathbf{z}_\alpha), \\ \text{s. t.} \quad & \sum_{\alpha=1}^P y_\alpha \mathbf{z}_\alpha = \mathbf{b} - \mathcal{P}\mathbf{n}_g, \\ & \sum_{\alpha=1}^P y_\alpha = \tilde{b} - \mathbf{e}_{n+1}^T \mathbf{n}_g, \\ & y_\alpha \geq 0, \quad \alpha = 1, \dots, P, \\ & \mathbf{z}_\alpha \in \text{int}\Delta_n, \quad \alpha = 1, \dots, P. \end{aligned} \tag{8}$$

After scaling the variables y_α , the solution to (8) is the unique value of the convex envelope of the function f at point $(\tilde{b} - \mathbf{e}_{n+1}^T \mathbf{n}_g)^{-1}(\mathbf{b} - \mathcal{P}\mathbf{n}_g)$:

$$\begin{aligned}
& (\text{conv}f)((\tilde{\mathbf{b}} - \mathbf{e}_{n+1}^T \mathbf{n}_g)^{-1}(\mathbf{b} - \mathcal{P}\mathbf{n}_g)) = \\
& \inf \left\{ \sum_{\alpha=1}^P y_\alpha f(\mathbf{z}_\alpha) \left| \sum_{\alpha=1}^P y_\alpha \mathbf{z}_\alpha = (\tilde{\mathbf{b}} - \mathbf{e}_{n+1}^T \mathbf{n}_g)^{-1}(\mathbf{b} - \mathcal{P}\mathbf{n}_g), y_\alpha \geq 0, \sum_{\alpha=1}^P y_\alpha = 1 \right. \right\}.
\end{aligned}$$

This global minimizer is well-defined and unique [2, 36]. Therefore $\mathcal{H}(\mathbf{n}_g)$ is a convex function of \mathbf{n}_g and (7) is an unconstrained convex minimization problem that admits a unique global minimizer. \blacksquare

According to the *Carathéodory theorem* [37], the number of phases P is bounded by $n + 1$. An interior-point method is introduced to relax the inequality constraints $y_\alpha \geq 0$ by means of a log/barrier penalty term. Let us denote by $\nu \in \mathbb{R}_{++}$ the interior-point parameter. The relaxed minimization problem reads:

$$\begin{aligned}
\min \quad & \sum_{\alpha=1}^P y_\alpha f(\mathbf{z}_\alpha) + \mathbf{n}_g^T (\boldsymbol{\mu}_g(\mathbf{n}_g) - \mathbf{e}_{n+1}) - \sum_{\alpha=1}^P \nu \ln(y_\alpha), \\
\text{s. t.} \quad & \sum_{\alpha=1}^P y_\alpha \mathbf{z}_\alpha + \mathcal{P}\mathbf{n}_g = \mathbf{b}, \quad \sum_{\alpha=1}^P y_\alpha + \mathbf{e}_{n+1}^T \mathbf{n}_g = \tilde{\mathbf{b}}, \\
& \mathbf{z}_\alpha \in \text{int}\Delta_n, \quad \alpha = 1, \dots, P, \quad \mathbf{n}_g > 0.
\end{aligned} \tag{9}$$

Problem (9) is not equivalent to (6) since it contains only equality constraints. A primal-dual interior-point algorithm approximately solves (9) by applying one Newton iteration to its KKT system of equations, then decreasing ν and repeating the process. Since the objective function and constraints are continuous, the sequence of solutions of the penalized problem will converge to the solution of (6) as $\nu \rightarrow 0$ [16]. Let $L(\mathbf{n}_g, y_\alpha, \mathbf{z}_\alpha, \boldsymbol{\eta}, \gamma)$ be the Lagrangian function

$$\begin{aligned}
L(y_\alpha, \mathbf{z}_\alpha, \boldsymbol{\eta}, \gamma, \mathbf{n}_g) &= \sum_{\alpha=1}^P y_\alpha f(\mathbf{z}_\alpha) + \mathbf{n}_g^T (\boldsymbol{\mu}_g(\mathbf{n}_g) - \mathbf{e}_{n+1}) - \sum_{\alpha=1}^P \nu \ln(y_\alpha) \\
&+ \boldsymbol{\eta}^T \left(\sum_{\alpha=1}^P y_\alpha \mathbf{z}_\alpha + \mathcal{P}\mathbf{n}_g - \mathbf{b} \right) + \gamma \left(\sum_{\alpha=1}^P y_\alpha + \mathbf{e}_{n+1}^T \mathbf{n}_g - \tilde{\mathbf{b}} \right),
\end{aligned} \tag{10}$$

where $\boldsymbol{\eta} \in \mathbb{R}^n$ and $\gamma \in \mathbb{R}$ are the dual variables relative to the equality constraints. The first order optimality conditions (Karush-Kuhn-Tucker conditions) relative to (9) are equivalent to the solution of $\nabla L(\mathbf{n}_g, y_\alpha, \mathbf{z}_\alpha, \boldsymbol{\eta}, \gamma) = 0$, *i.e.* the stationary points of the Lagrangian function:

$$\begin{aligned}
& \boldsymbol{\mu}_g(\mathbf{n}_g) + \boldsymbol{\lambda} = \mathbf{0}, \\
& y_\alpha (\nabla f(\mathbf{z}_\alpha) + \boldsymbol{\eta}) = \mathbf{0}, \quad \alpha = 1, \dots, P, \\
& f(\mathbf{z}_\alpha) + \boldsymbol{\eta}^T \mathbf{z}_\alpha + \gamma - \frac{\nu}{y_\alpha} = 0, \quad \alpha = 1, \dots, P, \\
& \sum_{\alpha=1}^P y_\alpha \mathbf{z}_\alpha + \mathcal{P}\mathbf{n}_g = \mathbf{b}, \\
& \sum_{\alpha=1}^P y_\alpha + \mathbf{e}_{n+1}^T \mathbf{n}_g = \tilde{\mathbf{b}}.
\end{aligned} \tag{11}$$

where $\boldsymbol{\lambda} = (\boldsymbol{\eta}^T + \gamma \mathbf{e}_n^T, \gamma)^T \in \mathbb{R}^{n+1}$ is obtained by agglomerating the terms coming from the two multipliers $\boldsymbol{\eta}$ and γ , and the corresponding equality constraints (which implies that the derivative with respect to the last component of \mathbf{n}_g involves only one contribution, while those with respect to the first n involve contributions from both equality constraints). Note that the derivative of $\mathbf{n}_g^T (\boldsymbol{\mu}_g(\mathbf{n}_g) - \mathbf{e}_{n+1})$ is given by $\boldsymbol{\mu}_g(\mathbf{n}_g)$.

If $(\mathbf{n}_g^*, y_\alpha^*, \mathbf{z}_\alpha^*, \boldsymbol{\eta}^*, \gamma^*)$ is a KKT point solution of (11), the necessary second order conditions relative to (9) are given by

$$w^T \nabla_{xx}^2 L(\mathbf{n}_g^*, y_\alpha^*, \mathbf{z}_\alpha^*, \boldsymbol{\eta}^*, \gamma^*) w = w^T \begin{pmatrix} \mathbf{H}_g & \mathbf{0} & \mathbf{0} \\ \mathbf{0} & \mathbf{y} \nabla^2 f & \mathbf{0} \\ \mathbf{0} & \mathbf{0} & \nu / \mathbf{y}^2 \end{pmatrix} w \geq 0, \quad (12)$$

for all w satisfying constraint conditions (see [32] for instance), where $\mathbf{y} \nabla^2 f = \text{diag}(y_\alpha \nabla^2 f(\mathbf{z}_\alpha)) \in \mathbb{R}^{nP \times nP}$, $\nu / \mathbf{y}^2 = \text{diag}(\nu / y_\alpha^2) \in \mathbb{R}^{P \times P}$, and $\mathbf{H}_g = \nabla \boldsymbol{\mu}_g(\mathbf{n}_g) = \text{diag}\left(\frac{1}{\mathbf{n}_{g,i}}\right)$. Therefore the second order conditions are satisfied if the diagonal blocks of (12) are positive definite. This is always the case for the first and third diagonal block. The necessary second order conditions are therefore satisfied if $\mathbf{y} \nabla^2 f \geq 0$.

Lemma 2 *If the concentration vectors \mathbf{z}_α , $\alpha = 1, \dots, P$ are affinely independent, the linear independent constraint qualification (LICQ) holds for (11) at any feasible point.*

The proof of this lemma is similar to [2, 22].

Theorem 3 *A solution $(y_\alpha, \mathbf{z}_\alpha, \mathbf{n}_g)$ is a global minimum of (9) if and only if $(y_\alpha, \mathbf{z}_\alpha, \mathbf{n}_g, \boldsymbol{\eta}, \gamma)$ is a KKT point of (11) with $\mathbf{z}_\alpha \in \Delta_n$ such that $\nabla^2 f(\mathbf{z}_\alpha) > 0$ and $y_\alpha > 0$.*

Proof. Under the given assumptions, the sufficient second order conditions are satisfied [32]. The property $\nabla^2 f(\mathbf{z}_\alpha) > 0$ implies not only that the second order sufficient optimality conditions are satisfied, but also that the solution to (8) is the value of the convex envelope of f , which is the global optimum by use of the tangent plane criterion [26, 30]. The convexity of the objective function in (7) implies that the global optimum in the variables \mathbf{n}_g is unique and the local minimum is also the global one. \blacksquare

The KKT system that arises when applying a Newton step to the system of first order conditions (11) can be written as

$$\begin{pmatrix} \mathbf{H}_g & \mathbf{0} & \mathbf{0} & \mathbf{T}_\eta^T & \mathbf{T}_\gamma^T \\ \mathbf{0} & \mathbf{y} \nabla^2 f & \nabla f + \boldsymbol{\eta} & \mathbf{Y} & \mathbf{0} \\ \mathbf{0} & (\nabla f + \boldsymbol{\eta})^T & \nu / \mathbf{y}^2 & \mathbf{Z} & \mathbf{e}_P \\ \mathbf{T}_\eta & \mathbf{Y}^T & \mathbf{Z}^T & \mathbf{0} & \mathbf{0} \\ \mathbf{T}_\gamma & \mathbf{0} & \mathbf{e}_P^T & \mathbf{0} & \mathbf{0} \end{pmatrix} \begin{pmatrix} \mathbf{p}_g \\ \mathbf{p}_z \\ \mathbf{p}_y \\ \mathbf{p}_\eta \\ p_\gamma \end{pmatrix} = \begin{pmatrix} \mathbf{b}_g \\ \mathbf{b}_z \\ \mathbf{b}_y \\ \mathbf{b}_\eta \\ b_\gamma \end{pmatrix} \quad (13)$$

where the blocks of the system are defined by:

$$\begin{aligned} \mathbf{y} \nabla^2 f &= \text{diag}(y_\alpha \nabla^2 f(\mathbf{z}_\alpha)) \in \mathbb{R}^{nP \times nP}, & \nu / \mathbf{y}^2 &= \text{diag}(\nu / y_\alpha^2) \in \mathbb{R}^{P \times P}, \\ \nabla f + \boldsymbol{\eta} &= \text{diag}(\nabla f(\mathbf{z}_\alpha) + \boldsymbol{\eta}) \in \mathbb{R}^{nP \times P}, & \mathbf{Y} &= (y_1 \mathbf{I}_n, \dots, y_P \mathbf{I}_n)^T \in \mathbb{R}^{nP \times n}, \\ \mathbf{Z} &= (\mathbf{z}_1, \dots, \mathbf{z}_P) \in \mathbb{R}^{P \times n}, & \mathbf{H}_g &= \nabla \boldsymbol{\mu}_g(\mathbf{n}_g) = \text{diag}\left(\frac{1}{\mathbf{n}_{g,i}}\right) \end{aligned}$$

and

$$\mathbf{T} = \begin{pmatrix} \mathbf{T}_\eta \\ \mathbf{T}_\gamma \end{pmatrix} = \begin{pmatrix} \mathbf{I}_n & \mathbf{0} \\ \mathbf{e}_n^T & 1 \end{pmatrix} \in \mathbb{R}^{(n+1) \times (n+1)}.$$

The upper diagonal block matrix \mathbf{H}_g counts for the contributions from the gas phase. The solution of the linear system $\mathbf{p}_g, \mathbf{p}_z = (\mathbf{p}_{z_\alpha}), \mathbf{p}_y = (p_{y_\alpha}), \mathbf{p}_\eta, p_\gamma$ are the increments for the variables $\mathbf{n}_g, \mathbf{z}_\alpha, y_\alpha, \boldsymbol{\eta}, \gamma$ respectively. Finally, the right-hand sides $\mathbf{b}_g, \mathbf{b}_z = (\mathbf{b}_{z_\alpha}), \mathbf{b}_y = (b_{y_\alpha}), \mathbf{b}_\eta, b_\gamma$ are explicitly given by variations of [2]:

$$\begin{aligned} \mathbf{b}_g &= -(\boldsymbol{\mu}_g(\mathbf{n}_g) + \boldsymbol{\lambda}), \\ \mathbf{b}_{z_\alpha} &= -y_\alpha \nabla_{z_\alpha} f - y_\alpha \boldsymbol{\eta} - y_\alpha \mathbf{Z}_{\mathbf{e}_{n+1}}^T \nabla^2 g(\mathbf{x}_\alpha) \mathbf{p}_{\mathbf{x}_\alpha}^0 \\ &= -y_\alpha \nabla_{z_\alpha} f - y_\alpha \boldsymbol{\eta} - y_\alpha (1 - \mathbf{e}_{n+1}^T \mathbf{x}_\alpha) (\partial_{1:n_s, n_s}^2 g(\mathbf{x}_\alpha) - \partial_{n_s, n_s}^2 g(\mathbf{x}_\alpha) \mathbf{e}_n), \quad \alpha = 1, \dots, P, \\ b_{y_\alpha} &= -g(\mathbf{x}_\alpha) - \mathbf{x}_\alpha^T \boldsymbol{\lambda} + \nu y_\alpha^{-1} - (\nabla g(\mathbf{x}_\alpha) + \boldsymbol{\lambda})^T \mathbf{p}_{\mathbf{x}_\alpha}^0 \\ &= -g(\mathbf{x}_\alpha) - \mathbf{x}_\alpha^T \boldsymbol{\lambda} + \nu y_\alpha^{-1} - (1 - \mathbf{e}_{n+1}^T \mathbf{x}_\alpha) (\partial_{n_s} g(\mathbf{x}_\alpha) + \boldsymbol{\lambda}_{n_s}), \quad \alpha = 1, \dots, P, \\ \mathbf{b}_\eta &= \mathbf{b} - \sum_{\alpha=1}^P y_\alpha \mathbf{z}_\alpha - \mathcal{P} \mathbf{n}_g \\ b_\gamma &= \tilde{b} - \sum_{\alpha=1}^P y_\alpha - \mathbf{e}_{n+1}^T \mathbf{n}_g. \end{aligned}$$

where $\mathbf{Z}_{\mathbf{e}_{n+1}} = \begin{pmatrix} \mathbf{I}_n \\ -\mathbf{e}_n^T \end{pmatrix} \in \mathbb{R}^{n+1 \times n}$ is the null-space matrix such that $\mathbf{Z}_{\mathbf{e}_{n+1}}^T \mathbf{e}_{n+1} = \mathbf{0}$.

The primal-dual interior-point algorithm for the computation of equilibrium consists in solving (13) for given parameter ν , before decreasing the value of the interior-point parameter. It is sketched as follows:

- Initialization of $y_\alpha^0, \mathbf{z}_\alpha^0, \boldsymbol{\eta}^0, \gamma^0, \mathbf{n}_g^0$ and ν^0 .
- For $j = 0, 1, 2, \dots$
 1. Compute the reduced Newton direction $(\mathbf{p}_g, \mathbf{p}_z, \mathbf{p}_y, \mathbf{p}_\eta, p_\gamma)$ by solving *one* step of the Newton method and (13).
 2. Compute a reduced step-length τ to ensure that $y_\alpha^{j+1} = y_\alpha^j + \tau p_{y_\alpha} > 0$ and $g(\mathbf{x}_\alpha^j + \tau p_{\mathbf{x}_\alpha}) + (\mathbf{x}_\alpha^j + \tau p_{\mathbf{x}_\alpha})^T (\boldsymbol{\lambda}^j + \tau p_\lambda) \geq 0$ for all $\alpha = 1, \dots, P$, and to force the decrease of some merit function to obtain feasible iterates (see Section 4).
 3. Update $\mathbf{n}_g^{j+1}, y_\alpha^{j+1}, \mathbf{z}_\alpha^{j+1} (\alpha = 1, \dots, P), \boldsymbol{\eta}^{j+1}$ and γ^{j+1} .
 4. For all pairs α, α' , merge \mathbf{z}_α^{j+1} and $\mathbf{z}_{\alpha'}^{j+1}$ into one phase if $\left\| \mathbf{z}_\alpha^{j+1} - \mathbf{z}_{\alpha'}^{j+1} \right\|_2$ is smaller than a given tolerance.
 5. Compute the new parameter ν^{j+1} .
 6. Compute the discrepancy associated to the computed increments and stop if some stopping criterion is satisfied. Otherwise, go to 1.

The merging step in the previous algorithm avoids spurious solutions with two mole-fractions \mathbf{z}_α with similar compositions. Due to the geometry of the problem, the convex regions of f are known to be in the neighborhood of the corners of the simplex. The algorithm enforces the mole-fraction \mathbf{z}_α to remain in the convex regions of the function f , as long as convex regions are separated. However, due to the topology of f , the different vectors \mathbf{z}_α may merge when they end up in the same convex region. Two vectors \mathbf{z}_α and $\mathbf{z}_{\alpha'}$ having similar compositions in the sense of a small Euclidean distance are aggregated into one phase. The total mass of the resulting phase is defined as the sum of the masses in the aggregated phases. The aggregation of two phases allows to keep only linearly independent constraints, but could prevent the algorithm to converge to the global optimum when done too quickly. One has to avoid this wrong situation by enforcing the phases to remain in disjoint convex regions whenever possible. Numerical experiments have shown that the deactivation of a phase α is usually due to the constraint $y_\alpha = 0$, before the corresponding mole-fraction \mathbf{z}_α actually merges with another phase.

Non-empty phases are defined as the phases α such that $y_\alpha > 0$, and correspond to the phases that contains a strictly positive amount of moles of chemical species. The accurate identification of non-empty phases is important (see *e.g.* [15]). Such an identification reduces the inequality constrained minimization problem to an equality constrained problem which is much easier to deal with. A phase identification procedure that correctly detects non-empty phases in a neighborhood of a KKT point is incorporated to the present algorithm. The primal-dual interior-point algorithm will produce a sequence of sets \mathcal{A} (resp. \mathcal{E}) of non-empty phases (resp. empty phases). The main criterion for filling phases will be the value of the corresponding variables y_α . We use the identification function

$$\rho(y_\alpha, \mathbf{z}_\alpha, \zeta_\alpha, \boldsymbol{\eta}, \gamma, \mathbf{n}_g) := \left\| \nabla_{(y_\alpha, \mathbf{z}_\alpha, \zeta_\alpha, \boldsymbol{\eta}, \gamma, \mathbf{n}_g)} L(y_\alpha, \mathbf{z}_\alpha, \boldsymbol{\eta}, \gamma, \mathbf{n}_g) \right\|, \quad (14)$$

where L is the Lagrangian function defined by (10). The function ρ is continuous and vanishes at any solution of (11) (KKT point). The numerical experience has shown that this identification function allows a correct identification of the non-empty/empty phases. The index set of vanishing phases is defined by $\mathcal{E} := \{ \alpha \mid y_\alpha \leq c \rho(y_\alpha, \mathbf{z}_\alpha, \boldsymbol{\eta}, \gamma, \mathbf{n}_g) \}$, with $c > 0$ is a given constant. The set \mathcal{E} gives the vanishing phases such that y_α is close to zero, coupled with the information that $(y_\alpha, \mathbf{z}_\alpha, \boldsymbol{\eta}, \gamma, \mathbf{n}_g)$ is sufficiently close to a KKT point [15]. The set \mathcal{A} of active constraints (non-empty phases) can subsequently be defined by the complementary set:

$$\mathcal{A} := \{1, \dots, P\} \setminus \mathcal{E}. \quad (15)$$

The interior-point method is coupled with this active set method for the activation/deactivation of the inequality constraints. Starting with $\mathcal{A}^0 = \{1, \dots, P\}$, the active set of non-empty phases \mathcal{A}^j is computed by (15) at each iteration j . The problem (11) is projected on the reduced set of active constraints and solved with a Newton method to give a new iterate $(y_\alpha^{j+1}, \mathbf{z}_\alpha^{j+1}, \boldsymbol{\eta}^{j+1}, \gamma^{j+1}, \mathbf{n}_g^{j+1})$.

The sets \mathcal{A}^j and \mathcal{E}^j are updated at each iteration. Let \mathcal{P}^a denote the index set of phases $\alpha \in \mathcal{A}^j$, that satisfy $y_\alpha^{j+1} \leq c \rho(y_\alpha^{j+1}, \mathbf{z}_\alpha^{j+1}, \boldsymbol{\eta}^{j+1}, \gamma^{j+1}, \mathbf{n}_g^{j+1})$ or $0 < y_\alpha^{j+1} < \varepsilon_y$, where ε_y is a fixed threshold (set to 10^{-8} in practice). The set \mathcal{P}^a represents the set of inequality constraints that are deactivated at the next iteration.

On the other hand, let \mathcal{P}^d denote the index set of phases $\alpha \notin \mathcal{A}^j$, that satisfy $g(\mathbf{x}_\alpha^{j+1}) + (\mathbf{x}_\alpha^{j+1})^T \boldsymbol{\lambda}^{j+1} < 0$ (the distance between the tangent plane and the graph of the objective function at point \mathbf{x}_α^+ is negative). According to the tangent plane criterion [26, 30], this set denotes the inactive constraints that have to be added to the active set. The new active set \mathcal{A}^{j+1} is then given at the next iteration by

$$\mathcal{A}^{j+1} = \left(\mathcal{A}^j \cup \mathcal{P}^d \right) \setminus \mathcal{P}^a. \quad (16)$$

The KKT equations (11) are then projected on the new set \mathcal{A}^{j+1} and another Newton iteration is carried out.

Note that, by removing inactive phases from the set of equations, the active-set procedure (16) prevents the search direction from obtaining unfeasible iterates, as emphasized in [44] for (even simple) non-convex equality constraints. The sequence of iterates generated is asymptotically a sequence of feasible iterates, as shown in the numerical experiments presented in Section 5.

The interior-point algorithm for the resolution of (11) described previously is coupled with the active-sets determination and reads as follows:

- Initialization of $y_\alpha^0, \mathbf{z}_\alpha^0, \boldsymbol{\eta}^0, \gamma^0, \mathbf{n}_g^0$ and $\nu = \nu^0$. Set $\mathcal{A}^0 = \{1, \dots, P\}$.
- For $j = 0, 1, 2, \dots$
 1. Compute the reduced Newton direction $(\mathbf{p}_g, \mathbf{p}_{\mathbf{z}_\alpha}, p_{y_\alpha}, \mathbf{p}_\eta, p_\gamma)$ by solving *one* step (13) of the Newton method associated with the active set \mathcal{A}^j .
 - (a) Compute first \mathbf{p}_g as described in Section 3.
 - (b) Compute $(\mathbf{p}_{\mathbf{z}_\alpha}, \mathbf{p}_{y_\alpha}, \mathbf{p}_\eta, p_\gamma)$ (for given \mathbf{p}_g) by solving the lower right block of (13) as described in [2].
 2. Compute a reduced step-length τ to ensure that $y_\alpha^{j+1} = y_\alpha^j + \tau p_{y_\alpha} > 0$ and $g(\mathbf{x}_\alpha^j + \tau p_{\mathbf{x}_\alpha}) + (\mathbf{x}_\alpha^j + \tau p_{\mathbf{x}_\alpha})^T (\boldsymbol{\lambda}^j + \tau p_\lambda) \geq 0$ for all $\alpha = 1, \dots, P$.
 3. Update $\mathbf{n}_g^{j+1}, y_\alpha^{j+1}, \mathbf{z}_\alpha^{j+1} (\alpha = 1, \dots, P), \boldsymbol{\eta}^{j+1}$ and γ^{j+1} .
 4. For all pairs α, α' , merge \mathbf{z}_α^{j+1} and $\mathbf{z}_{\alpha'}^{j+1}$ into one phase if $\left\| \mathbf{z}_\alpha^{j+1} - \mathbf{z}_{\alpha'}^{j+1} \right\|_2$ is smaller than a given tolerance.
 5. Update the set of non-empty phases \mathcal{A}^{j+1} , and compute the new parameter ν^{j+1} .
 6. Compute the discrepancy associated to the computed increments and stop if some stopping criterion is satisfied. Otherwise, go to 1.

In the sequel, the resolution method for the linear system (13) is detailed and justified. A reduced space decomposition approach is developed. It allows to avoid approximation errors introduced by iterative methods, resolves the poor condition number of the matrix arising in (13), and takes advantage of the sparsity of the matrix $\mathbf{y} \nabla^2 f$ that is block diagonal (with each diagonal block having very different eigenvalues).

3 A Sequential Quadratic Programming Interior-Point Method

The resolution of the KKT system relies on the interior-point method with one Newton iteration. The linear system corresponding to the pure liquid-liquid equilibrium appears in the lower right block of (13). For gas-liquid partitioning, the gas concentration participates to the Gibbs free energy and leads to an *augmented* linear system.

We split the sub-problem relative to the gas phase from the one coming from the liquid phases with a sequential quadratic programming (SQP) approach. The objective is to control the inertia of the system, and to incorporate the interior-point method designed in [2] in the resolution of (13) at each iteration of the interior-point procedure.

The design of such linear algebra techniques is needed for the following reasons. Keeping in mind that the number of chemical species can be large, solution techniques based on iterative methods are intractable due to the poor condition number of the matrix (13). Indeed, the eigenvalues of \mathbf{H}_g and those of the diagonal blocks of $\mathbf{y}\nabla^2 f$ are very different and lead to condition numbers that may reach 10^{13} for $n = 3$ only. The reasons for such a poor condition number come from the extreme diversity of the concentrations, that can range over many orders of magnitude, and from the topology of the energy function f , that allows very large gradients and ill-conditioned Hessians, especially near the boundaries of the simplex Δ_n . Direct decomposition methods allow to take into account the sparsity of the matrix and save on memory requirements when the number of chemical species n becomes large.

A sequential quadratic programming method allows to write the KKT system (13) as a quadratic minimization problem for the increments $\mathbf{p}_{\mathbf{z}_\alpha}, p_{y_\alpha}, \mathbf{p}_\eta, p_\gamma$ and \mathbf{p}_g . Let us describe briefly the local sequential quadratic programming approach, as in [32], for the resolution of (9). We use the model problem

$$\min_{X \in \mathbb{R}^N} F(X) \quad \text{such that} \quad C(X) = 0$$

where, in (9), $X := (\mathbf{z}_\alpha, y_\alpha, \mathbf{n}_g)$, $N = n + 1 + (n + 1)P + P$, $F(X) = \sum_{\alpha=1}^P y_\alpha f(\mathbf{z}_\alpha) + \mathbf{n}_g^T (\boldsymbol{\mu}_g(\mathbf{n}_g) - \mathbf{e}_{n+1}) - \sum_{\alpha=1}^P \nu \ln(y_\alpha)$ and $C(X) = (\sum_{\alpha=1}^P y_\alpha \mathbf{z}_\alpha + \mathcal{P} \mathbf{n}_g - \mathbf{b}, \sum_{\alpha=1}^P y_\alpha + \mathbf{e}_{n+1}^T \mathbf{n}_g - \tilde{b})^T$.

The increments of the Newton method are denoted by $d := (\mathbf{p}_{\mathbf{z}_\alpha}, \mathbf{p}_{y_\alpha}, \mathbf{p}_{\mathbf{n}_g})$. For a given KKT point (X^*, λ^*) , the determination of d with a local SQP approach consist in solving

$$\min_{d \in \mathbb{R}^N} \nabla F(x)^T d + \frac{1}{2} d^T \nabla_{XX}^2 L(X^*, \lambda^*) d \quad \text{such that} \quad C(X^*) + \nabla C(X^*)^T d = 0$$

where the Lagrangian function $L(X, \lambda)$ is defined by (10). This problem for the increments d can be solved by seeking stationary points of the corresponding Lagrangian. The local SQP approach for the problem (9) is therefore equivalent to the following minimization problem:

$$\begin{aligned}
\min_{\mathbf{p}_{\mathbf{z}_\alpha}, p_{y_\alpha}, \mathbf{p}_g} \quad & \frac{1}{2} \mathbf{p}_g^T \mathbf{H}_g \mathbf{p}_g + \frac{1}{2} \sum_{\alpha=1}^P (\mathbf{p}_{\mathbf{z}_\alpha} \ p_{y_\alpha})^T \begin{pmatrix} y_\alpha \nabla^2 f(\mathbf{z}_\alpha) & (\nabla f(\mathbf{z}_\alpha) + \boldsymbol{\eta}) \\ (\nabla f(\mathbf{z}_\alpha) + \boldsymbol{\eta})^T & \frac{\nu}{y_\alpha^2} \end{pmatrix} \begin{pmatrix} \mathbf{p}_{\mathbf{z}_\alpha} \\ p_{y_\alpha} \end{pmatrix} \\
& + \sum_{\alpha=1}^P (\mathbf{b}_{\mathbf{z}_\alpha} - y_\alpha \boldsymbol{\eta} \quad b_{y_\alpha} - \mathbf{z}_\alpha^T \boldsymbol{\eta} - (\mathbf{e}_{n+1}^T \mathbf{x}_\alpha) \gamma)^T \begin{pmatrix} \mathbf{p}_{\mathbf{z}_\alpha} \\ p_{y_\alpha} \end{pmatrix} - \mathbf{b}_g^T \mathbf{p}_g \\
\text{s. t.} \quad & \sum_{\alpha=1}^P (\mathbf{e}_{n+1}^T \mathbf{x}_\alpha) p_{y_\alpha} + \mathbf{T}_\gamma \mathbf{p}_g = b_\gamma, \quad \sum_{\alpha=1}^P y_\alpha \mathbf{p}_{\mathbf{z}_\alpha} + \sum_{\alpha=1}^P \mathbf{z}_\alpha p_{y_\alpha} + \mathbf{T}_\eta \mathbf{p}_g = \mathbf{b}_\eta
\end{aligned} \tag{17}$$

When separating the variable \mathbf{p}_g from the other increments, the local SQP problem (17) is equivalent to:

$$\min_{\mathbf{p}_g} \left\{ \frac{1}{2} \mathbf{p}_g^T \mathbf{H}_g \mathbf{p}_g - \mathbf{b}_g^T \mathbf{p}_g + \mathcal{G}(\mathbf{p}_g) \right\}, \tag{18}$$

where $\mathcal{G}(\mathbf{p}_g)$ is the optimum value (function of \mathbf{p}_g) of the minimization problem defined by

$$\begin{aligned}
\min_{\mathbf{p}_{\mathbf{z}_\alpha}, p_{y_\alpha}} \quad & \frac{1}{2} \sum_{\alpha=1}^P (\mathbf{p}_{\mathbf{z}_\alpha} \ p_{y_\alpha})^T \begin{pmatrix} y_\alpha \nabla^2 f(\mathbf{z}_\alpha) & (\nabla f(\mathbf{z}_\alpha) + \boldsymbol{\eta}) \\ (\nabla f(\mathbf{z}_\alpha) + \boldsymbol{\eta})^T & \frac{\nu}{y_\alpha^2} \end{pmatrix} \begin{pmatrix} \mathbf{p}_{\mathbf{z}_\alpha} \\ p_{y_\alpha} \end{pmatrix} \\
& + \sum_{\alpha=1}^P (\tilde{\mathbf{b}}_{\mathbf{z}_\alpha} \ \tilde{b}_{y_\alpha})^T \begin{pmatrix} \mathbf{p}_{\mathbf{z}_\alpha} \\ p_{y_\alpha} \end{pmatrix} \\
\text{s. t.} \quad & \sum_{\alpha=1}^P (\mathbf{e}_{n+1}^T \mathbf{x}_\alpha) p_{y_\alpha} = b_\gamma - \mathbf{T}_\gamma \mathbf{p}_g, \quad \sum_{\alpha=1}^P y_\alpha \mathbf{p}_{\mathbf{z}_\alpha} + \sum_{\alpha=1}^P \mathbf{z}_\alpha p_{y_\alpha} = \mathbf{b}_\eta - \mathbf{T}_\eta \mathbf{p}_g
\end{aligned} \tag{19}$$

where $\tilde{\mathbf{b}}_{\mathbf{z}_\alpha} = \mathbf{b}_{\mathbf{z}_\alpha} - y_\alpha \boldsymbol{\eta}$, and $\tilde{b}_{y_\alpha} = b_{y_\alpha} - \mathbf{z}_\alpha^T \boldsymbol{\eta} - (\mathbf{e}_{n+1}^T \mathbf{x}_\alpha) \gamma$. Note that the Hessian matrix \mathbf{H}_g relative to the introduction of the gas phase is diagonal and strictly positive definite, the gas concentrations being strictly positive.

In order to perform the following resolution method, we make the following classical assumptions:

(H5) The reduced Hessian $y_\alpha \nabla^2 f(\mathbf{z}_\alpha)$ is positive definite, for all $\alpha = 1, \dots, P$ (*i.e.* the sufficient second order optimality conditions hold).

(H6) The concentration vectors \mathbf{z}_α , $\alpha = 1, \dots, P$ are affinely independent (*i.e.* the LICQ condition holds).

Assumptions (H5) (H6) are required by the algorithm to encourage the primal-dual algorithm to converge to a stable equilibrium rather than any other first order optimality point such as a maximum, a saddle point, or a unstable local minimum [48]. Assumption (H5) is the mathematical translation of (H4). If (H5) is not satisfied, it is enforced by convexifying the reduced Hessian, so that the iterates \mathbf{z}_α generated by the method satisfy (H5). If (H6) is not satisfied, the affinely dependent mole-fractions concentration vectors \mathbf{z}_α that represent the same mixing of components are deleted in order to keep an affine independent set of vectors \mathbf{z}_α . In

liquid-liquid equilibria calculations in atmospheric chemistry, usually $P \ll n + 1$. However the algorithm handles the case $P = n + 1$, by enforcing the vectors \mathbf{z}_α to stay in disjoint convex regions whenever the topology of f makes it possible. It is practically observed that the phase \mathbf{z}_α is removed from the active set (and from the computations) since the corresponding variable y_α is vanishing, before the affine independence is lost.

First the explicit solution of the minimizer of $\mathcal{G}(\mathbf{p}_g)$ is expressed as a function of the gas concentrations \mathbf{p}_g . Then we solve the convex unconstrained minimization problem (18), whose minimizer is the solution of its first order optimality conditions. Finally, for \mathbf{p}_g given, the optimization problem (19) is solved with the techniques presented in [1, 2].

The following result is a direct consequence of the local sequential quadratic programming approach. Its proof is technical and can be found in Appendix A. The purpose of the proof is to provide a constructive determination of the increments and an actual description of the solver.

Theorem 4 *In a neighborhood of a KKT point, the displacements $\mathbf{p}_{\mathbf{z}_\alpha}$, $\alpha = 1, \dots, P$ and $\mathbf{p}_y = (\mathbf{p}_{y_\alpha})_{\alpha=1}^P$ in (19) are linear functions of \mathbf{p}_g , i.e.*

$$\mathbf{p}_y = \tilde{\mathbf{A}}_y \mathbf{p}_g + \tilde{\mathbf{B}}_y \quad (20)$$

$$\mathbf{p}_{\mathbf{z}_\alpha} = \tilde{\mathbf{A}}_{\mathbf{z}_\alpha} \mathbf{p}_g + \tilde{\mathbf{B}}_{\mathbf{z}_\alpha}, \quad \alpha = 1, \dots, P. \quad (21)$$

The displacements $\mathbf{p}_{\mathbf{z}_\alpha}$, \mathbf{p}_y are therefore linear functions of \mathbf{p}_g and similar technical calculations lead to the same conclusion for p_γ and \mathbf{p}_η .

Theorem 5 *In a neighborhood of a KKT point, the sequential quadratic programming problem (18) can be expressed as*

$$\begin{aligned} \mathbf{p}_g = \arg \min_{\mathbf{p}_g} & \quad \frac{1}{2} \mathbf{p}_g^T \left[\mathbf{H}_g + \tilde{\mathbf{A}}_y^T \left(\frac{\nu}{\mathbf{y}^2} \right) \tilde{\mathbf{A}}_y + \sum_{\alpha=1}^P \tilde{\mathbf{A}}_{\mathbf{z}_\alpha}^T y_\alpha \mathbf{H}_\alpha \tilde{\mathbf{A}}_{\mathbf{z}_\alpha} \right] \mathbf{p}_g \\ & + \mathbf{p}_g^T \left[-\mathbf{b}_g^T + \tilde{\mathbf{A}}_y^T \left(\frac{\nu}{\mathbf{y}^2} \right) \tilde{\mathbf{B}}_y + \sum_{\alpha=1}^P \tilde{\mathbf{A}}_{\mathbf{z}_\alpha} \tilde{\mathbf{b}}_{\mathbf{z}_\alpha} + \sum_{\alpha=1}^P \tilde{\mathbf{A}}_{\mathbf{z}_\alpha}^T y_\alpha \mathbf{H}_\alpha \tilde{\mathbf{B}}_{\mathbf{z}_\alpha} + \tilde{\mathbf{A}}_y^T \mathbf{b}_y \right]. \end{aligned} \quad (22)$$

Proof. Conclusion is obtained by inserting the expressions obtained in Theorem 4 into (18) and (19). ■

Theorem 6 *The problem (22) is a convex unconstrained minimization problem and admits a unique global minimizer \mathbf{p}_g , which is given by:*

$$\begin{aligned} \mathbf{p}_g = & - \left[\mathbf{H}_g + \tilde{\mathbf{A}}_y^T \left(\frac{\nu}{\mathbf{y}^2} \right) \tilde{\mathbf{A}}_y + \sum_{\alpha=1}^P \tilde{\mathbf{A}}_{\mathbf{z}_\alpha}^T y_\alpha \mathbf{H}_\alpha \tilde{\mathbf{A}}_{\mathbf{z}_\alpha} \right]^{-1} \times \\ & \left[-\mathbf{b}_g^T + \tilde{\mathbf{A}}_y^T \left(\frac{\nu}{\mathbf{y}^2} \right) \tilde{\mathbf{B}}_y + \sum_{\alpha=1}^P \tilde{\mathbf{A}}_{\mathbf{z}_\alpha} \tilde{\mathbf{b}}_{\mathbf{z}_\alpha} + \sum_{\alpha=1}^P \tilde{\mathbf{A}}_{\mathbf{z}_\alpha}^T y_\alpha \mathbf{H}_\alpha \tilde{\mathbf{B}}_{\mathbf{z}_\alpha} + \tilde{\mathbf{A}}_y^T \mathbf{b}_y \right]. \end{aligned} \quad (23)$$

Proof. The matrix \mathbf{H}_g is strictly positive definite and the additional contributions are positive semi-definite. The problem (22) is a strictly convex, unconstrained, minimization problem. The minimizer is given by the first order necessary KKT conditions (23). ■

Once the gas displacements \mathbf{p}_g have been computed with (22), the organic displacements $\mathbf{p}_{\mathbf{z}_\alpha}, p_{y_\alpha}, \mathbf{p}_\eta, p_\gamma$ can be computed by solving the KKT system corresponding to the minimization problem (19), with the techniques given in [2].

Corollary 7 *Due to the non-convex objective function and non-convex equality constraints, the convergence to the global optimum cannot be guaranteed (see e.g. [44]). On the other hand, the similar method applied in [2] to the liquid-liquid equilibrium system does converge to the global equilibrium. The gas-particle system being a small perturbation of the liquid-liquid equilibrium, this gives a strong incentive to develop a similar approach coupled with an appropriate initialization procedure that guarantees the algorithm to start "close" to the global minimum.*

The initialization technique mentioned above is developed in the next section.

4 Initialization Procedure

A technique for the initialization of the interior-point technique without the gas phase has been proposed in [2]. Starting from a good initial guess is crucial to favor the convergence of a Newton method to the global optimum of the energy, instead of a local minimum.

We present here an initialization procedure that is based on the geometric interpretation of the minimization problem as the determination of the convex envelope of the energy function and that relies on the location of the regions where the energy function f is convex. A two-step least-squares procedure that splits the liquid and the gas phases in a first approximation allows to extend the initialization to the gas-particle partitioning.

For a given feed vector $\bar{\mathbf{b}}$ we initialize the minimization process for the resolution of (6) as follows. The mole fractions $\bar{\mathbf{z}}_\alpha^0$ are initialized in a neighborhood $\Delta_n \cap \mathcal{N}$ of the vertices of Δ_n where the function f is convex and $\nabla^2 f(\bar{\mathbf{z}}_\alpha^0) > 0$. The variables \bar{y}_α^0 are the barycentric coordinates of $\bar{\mathbf{b}}$ in terms of $\bar{\mathbf{z}}_\alpha^0$. The dual variables $\boldsymbol{\lambda}^0$ are obtained from (11) in a least-squares sense by setting $\boldsymbol{\eta}^0 = \sum_{\alpha=1}^{n+1} y_\alpha \nabla f(\bar{\mathbf{z}}_\alpha^0)$ and $\gamma^0 = -\sum_{\alpha=1}^{n+1} (y_\alpha f(\bar{\mathbf{z}}_\alpha^0) + (\bar{\mathbf{z}}_\alpha^0)^T \boldsymbol{\eta}^0) + \nu^0(n+1)$.

Starting from this point, (11), with its first relation dismissed and $\mathbf{n}_g = \boldsymbol{\mu}_g = 0$, is solved with the interior-point technique discussed in [2]. A first approximation $(\mathbf{z}_\alpha^I, y_\alpha^I, \boldsymbol{\eta}^I, \gamma^I)$ is obtained. Since the points $\bar{\mathbf{z}}_\alpha^0$ are initialized such that the property $\nabla^2 f(\bar{\mathbf{z}}_\alpha^0) > 0$ is satisfied for all $\alpha = 1, \dots, n+1$, $(\mathbf{z}_\alpha^I, y_\alpha^I, \boldsymbol{\eta}^I, \gamma^I)$ is the global optimum of energy in the case $\mathbf{n}_g = \boldsymbol{\mu}_g = 0$. Assumption (H5) is satisfied and \mathbf{z}_α^I belongs to a convex region of f , since the method proposed in [2] ensures that property (with a convexification of the Hessian $y_\alpha \nabla^2 f(\mathbf{z}_\alpha)$ if needed).

Next an initial approximation of the quantity in the gas is determined. Given the dual parameter $\boldsymbol{\lambda}^I = (\boldsymbol{\eta}^I + \gamma^I \mathbf{e}_n, \gamma^I)^T$ and (11), the initial gas concentrations \mathbf{n}_g^0 are based on the relation $\boldsymbol{\mu}_g(\mathbf{n}_g^0) = \ln \left(\frac{\mathbf{n}_g^0 R T}{p_{\text{vapor}}} \right) = -\boldsymbol{\lambda}^I = - \begin{pmatrix} \boldsymbol{\eta}^I + \gamma^I \mathbf{e}_n \\ \gamma^I \end{pmatrix}$, where p_{vapor} is the given vector of vapor pressures corresponding to the corresponding chemical species [35], $R = 8.20575 \cdot 10^{-5}$ [$\text{m}^3 \text{ atm K}^{-1}$] is the gas constant and T is the ambient temperature. This relation leads to:

$$\mathbf{n}_g^0 = \frac{1}{RT} p_{\text{vapor}} \exp^{-\lambda^I}, \quad (24)$$

The partitioning between \mathbf{n}_g and $\bar{\mathbf{b}}$ is determined in the least-squares sense. Given the particle composition $\{\bar{y}_\alpha^I, \bar{\mathbf{x}}_\alpha^I\}$ and the gas concentrations \mathbf{n}_g^0 , the initial number of moles β^0 in the particle is given by the mass conservation relation

$$\mathbf{n}_g^0 + \beta^0 \sum_{\alpha=1}^P \bar{y}_\alpha^I \bar{\mathbf{x}}_\alpha^I = \bar{\mathbf{b}}. \quad (25)$$

This relation relies on the property of homogeneity for the concentrations in the liquid phases in the mass balance relation and objective function, which allows to scale the liquid quantities \bar{y}_α^I with the feed vector $\bar{\mathbf{b}}$ when $\mathbf{n}_g = 0$. However, the gas concentrations \mathbf{n}_g^0 are not scalable but fixed by (24). By multiplying (25) by $\bar{\mathbf{b}}^T$, the ratio β^0 and the final number of moles y_α^0 in the different phases can be obtained with $\beta^0 = \frac{\|\bar{\mathbf{b}}\|^2 - \bar{\mathbf{b}}^T \mathbf{n}_g^0}{\|\bar{\mathbf{b}}\|^2}$, $y_\alpha^0 = \beta^0 \bar{y}_\alpha^I$. The variables $\mathbf{x}_\alpha^0 = \bar{\mathbf{x}}_\alpha^I$ are unchanged since normalized. Assumption (H5) is therefore still satisfied at the end of the initialization process.

The coefficient β^0 is negative when one chemical component is only in the gas phase. This implies that (at least) one liquid phase disappears at equilibrium and the corresponding inequality constraint is an equality. When $\beta^0 < 0$, we correct (24) and set $\mathbf{n}_{g,i}^0 = \min\{\mathbf{n}_{g,i}^0, \bar{\mathbf{b}}_i - \varepsilon_{\beta^0}\}$ to restrict the gas concentrations to the maximal amount of each chemical (where $\varepsilon_{\beta^0} > 0$ is a small coefficient that guarantees the positiveness of $\sum_{\alpha=1}^P y_\alpha \mathbf{x}_\alpha$). The factor β^0 recomputed with the truncated \mathbf{n}_g^0 is positive. This initial guess is not necessary feasible with respect to the equality constraints.

The initial procedure described above provides the global optimum of the problem without the gas phase [2]. Therefore it also provides an initial guess that is in a small neighborhood of the global optimum of the combined problem (6). As a consequence, the algorithm proposed in this article shall be seen as a two-steps procedure involving an appropriate initialization of the complete problem with the solution of the simplified problem without gas phase. Numerical experiments in Section 5 will include both steps of the algorithm.

A line search method has been used in the active set approach to guarantee that the inequality constraints are satisfied for each iterate. The line-search method also allows to encourage convergence via a sufficient decrease in a merit function that encourages the early iterates to move towards the solution of the barrier problem (9). Let $\|\cdot\|_2$ denote the Euclidean norm. Our line-search method is based on the merit function [14] defined by

$$M_{\nu,\sigma}(y_\alpha, \mathbf{z}_\alpha, \mathbf{n}_g) = \sum_{\alpha=1}^P y_\alpha f(\mathbf{z}_\alpha) + \mathbf{n}_g^T (\boldsymbol{\mu}_g(\mathbf{n}_g) - \mathbf{e}_{n+1}) - \nu \sum_{\alpha=1}^P \ln(y_\alpha) + \frac{\sigma}{2} \left(\left\| \sum_{\alpha=1}^P y_\alpha \mathbf{z}_\alpha + \mathcal{P} \mathbf{n}_g - \mathbf{b} \right\|_2^2 + \left\| \sum_{\alpha=1}^P y_\alpha + \mathbf{e}_{n+1}^T \mathbf{n}_g - \tilde{b} \right\|_2^2 \right).$$

Our line-search method uses the solution of the KKT system (13) as a search direction. A sufficient decrease in $M_{\nu,\sigma}(y_\alpha, \mathbf{z}_\alpha, \mathbf{n}_g)$ is used to encourage progress towards a feasible solution and a minimizer of the penalized objective function.

The algorithm forces the approximations to be feasible at each iteration (up to rounding errors), except for the first iterates that may be unfeasible since the initialization process generates points that may be unfeasible and may violate the equality constraints. The method becomes a feasible method after a few iterations, as illustrated in Section 5. Therefore the minimization of M rapidly becomes equivalent to the minimization of the constrained problem, even if the merit function is not an exact penalty. From numerical experiments, the choice of a constant value for σ (*e.g.* $\sigma = 1$) is efficient enough to make the first iterates converges rapidly to a feasible solution that satisfies the equality constraints, as illustrated in Figure 3 in the next Section.

Let $\{y_i^\nu, \mathbf{z}_i^\nu, \mathbf{n}_g^\nu\}$ be the sequence of iterates generated by the interior-point method and define $\mathbf{b}^\nu = \sum_{i=1}^P y_i^\nu \mathbf{z}_i^\nu + \mathcal{P} \mathbf{n}_g^\nu$ and $\tilde{b}^\nu = \sum_{\alpha=1}^P y_\alpha^\nu + \mathbf{e}_{n+1}^T \mathbf{n}_g^\nu$. The convergence of the sequence $\{y_i^\nu, \mathbf{z}_i^\nu, \mathbf{n}_g^\nu\}$ to a local optimum happens under the sufficient second order optimality conditions. Given the initialization of the variables $\mathbf{z}_i^{\nu^0}$ in the convex regions of the function f , the value of the minimizer of (8) is the value of the convex envelope of f as long as $\nabla^2 f(\mathbf{z}_\alpha^\nu) > 0$. The addition of \mathbf{n}_g leads to a small perturbation of the convex envelope problem. However, since the perturbation is small, one can hope that the solution obtained by solving the convex envelope problem is close to the global optimum of the convex problem (7), and gives an appropriate initial guess for the modified problem.

The primal-dual interior-point method has two levels of inner and outer iterations, with the inner iterations corresponding to the iterations of Newton’s method for a given value of ν . If ν is reduced at an appropriate rate [18], the inner iterations can be terminated after one iteration.

5 Numerical Results

The primal-dual sequential quadratic programming interior-point algorithm is applied to the efficient prediction of the gas-particle partitioning of atmospheric aerosols under a large range of atmospheric conditions. Numerical examples of phase equilibrium problems are considered here to illustrate the efficiency of the algorithm.

5.1 Three Components System

We consider the three components system with 1-hexacosanol ($\text{C}_{26}\text{H}_{54}\text{O}$), pinic acid ($\text{C}_9\text{H}_{14}\text{O}_4$) and water (H_2O) at temperature 298.15 [K] and pressure 1 [atm]. This example of aerosol particles of atmospheric interest admits a maximum of three liquid phases at equilibrium for certain compositions. The dynamics of this system has been presented in [4], where the convergence to a stationary state has been shown. The vapor pressures p_{vapor} are given by 1.7734×10^{-5} , 2.2545×10^{-5} and 3.13×10^{-2} [atm] for 1-hexacosanol, pinic acid and water respectively. The initial value of the interior-point parameter is $\nu^0 = 10^{-3}$ and updated by $\nu^{k+1} = 0.7\nu^k$. One Newton iteration is performed before decreasing the interior-point parameter. A bad choice of the initial guess or another decrease of the interior-point parameter can lead the algorithm to select local minima or a saddle-point.

The stationary solution satisfies the equilibrium repartition of mass between gas and particle phases and the equilibrium mixing of components inside the particle. Numerical results are given in Table 1: the first case leads to a three liquid phases solution (*i.e.* all inequality constraints are strict inequalities), while the second case leads to a two liquid phases solution and the last

case to only one liquid phase. Each of them converge in 55 to 60 iterations for a tolerance of 10^{-13} on the residuals for the stopping criterion.

Table 1: Global optima for the water-hexacosanol-pinic acid system.

	Feed	Gas	Liquid	Liquid 1	Liquid 2	Liquid 3
$C_{26}H_{54}O$	2.0722d0	4.8648d-4	2.0717d0	2.3295d-3	3.4012d-12	6.0901d-1
$C_9H_{14}O_4$	2.3029d0	3.6465d-4	2.3026d0	3.7159d-1	3.3508d-3	2.1895d-1
H_2O	9.8165d0	1.2741d0	8.5424d0	6.2608d-1	9.9665d-1	1.7204d-1
y_α				4.1530d0	5.3778d0	3.3858d0
$C_{26}H_{54}O$	6.d0	4.9528d-4	5.9995d0	3.2918d-12	6.2688d-1	–
$C_9H_{14}O_4$	2.d0	3.4608d-4	1.9997d0	3.1347d-3	2.0627d-1	–
H_2O	11.d0	1.2743d0	9.7257d0	9.9687d-1	1.66834d-1	–
y_α				8.1546d0	9.5703d0	0.00d0
$C_{26}H_{54}O$	1.d0	8.3906d-4	9.9916d-1	5.0223d-2	–	–
$C_9H_{14}O_4$	10.d0	4.3410d-4	9.9996d0	5.0264d-1	–	–
H_2O	10.d0	1.1044.d0	8.8956d0	4.4714,d-1	–	–
y_α				19.89d0	0.00d0	0.00d0

Figures 1, 2 and 3 illustrate the results for $\bar{\mathbf{b}} = (2.072d0, 2.303d0, 9.817d0)$. Figure 1 shows the algorithm converges to stationary solutions for the gas-particle partitioning, as well as for the variables \mathbf{n}_g and y_α . The initialization procedure described in Section 4 gives an appropriate initial guess for the interior-point method. The iterates of the active set \mathcal{A} do not oscillate. Figure 2 shows the evolution of the variables \mathbf{z}_α , emphasizing that each of them remains in a neighborhood \mathcal{N} of each vertex of Δ_3 in which the sufficient second order optimality conditions are satisfied. Figure 3 shows the evolution of the objective and merit functions, showing that the iterations may be infeasible with respect to the equality constraints, and become feasible after a few iterations.

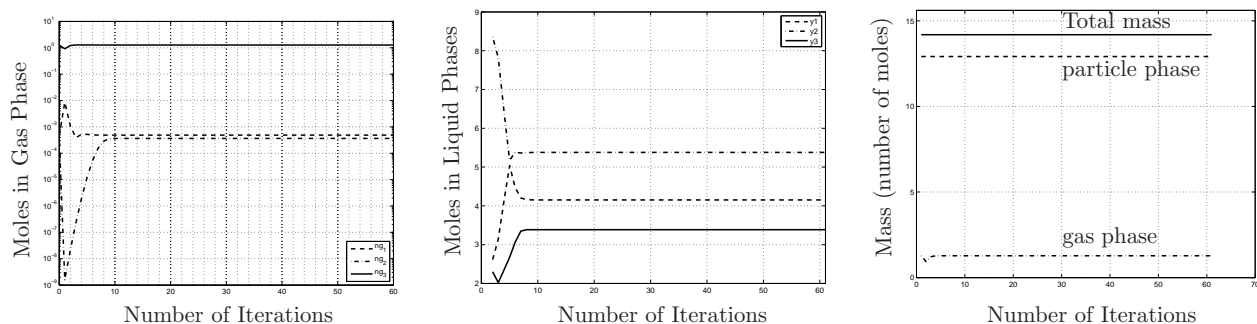


Figure 1: Convergence to a stationary point: components of \mathbf{n}_g on a logarithmic scale (left); variables y_α on a logarithmic scale (middle); conservation of mass on a logarithmic scale (right).

Results are compared with those obtained when the gas phase is not present (see [2]) in

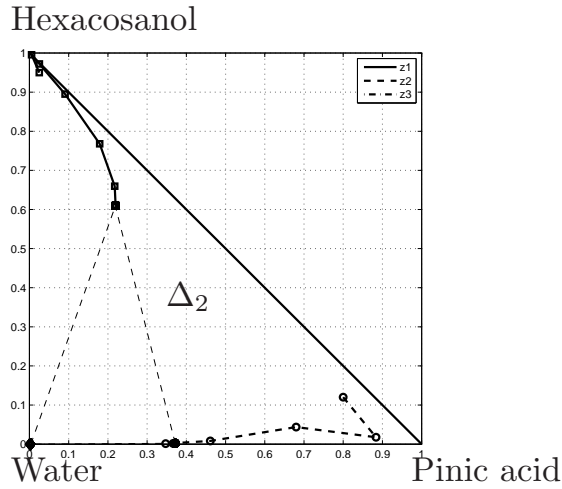


Figure 2: Convergence to a stationary point: convergence of the vertices \mathbf{z}_α .

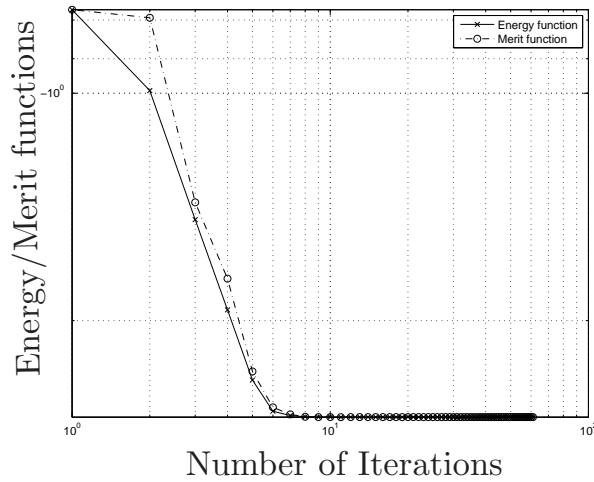


Figure 3: Evolution of energy and merit functions (log-log scale).

Table 2. The tolerance on the residual for stopping the interior-point method is 10^{-12} . The partitioning between gas and particle phases allows the system to lower its energy, compared to the situation with only liquid phases.

5.2 Two Components System

The scaling of the gas-particle partitioning is illustrated for the two components system with 1-hexacosanol and water. A solution with ratio 50% of water and 50% of hexacosanol is considered, the total number of moles varying from 4 to 4000 moles. Table 3 illustrates the numerical solution in terms of partitioning and number of iterations for both the interior-point method used for the

Table 2: Comparison between pure liquid equilibrium and gas-liquid partitioning for the water-hexacosanol-pinic acid system. Value of the objective function (energy of the system) and number of iterations of the algorithm (for the gas liquid equilibrium, the number of iterations into parenthesis is the number of iterations used in the initialization procedure).

Feed $\bar{\mathbf{b}}$	Liquid equilibrium		Gas-Liquid equilibrium	
	Objective	#iter.	Objective	#iter.
(4.d0 4.d0 16.d0)	-5.35103856	22	-5.35104211	13 (22)
(1.d0 1.d0 4.d0)	-1.33775964	22	-1.33776347	18 (22)
(1.d0 9.d0 25.d0)	-8.78692462	33	-8.80024880	17 (33)

initialization and the interior-point method used for the computation of the partitioning, with tolerance on the residuals equal to 10^{-6} . The results show that, given a similar initialization procedure, the number of iterations decreases with the number of moles in the system. The number of moles in the gas phase is constant, while the amount of moles in the liquid scales with the total amount of moles in the system. This shows that \mathbf{n}_g depends only on the slope λ of the tangent plane to the energy function (*i.e.* on the 50%-50% mixing between the chemical components) and is independent of the scaling factor of $\bar{\mathbf{b}}$.

Table 3: Sensitivity analysis of the gas-particle partitioning. Liquid and Gas concentrations of 1-hexacosanol and water respectively, and number of iterations for the interior-point method (in parenthesis: number of iterations for the initialization procedure).

Total Number of moles ($\mathbf{e}_{n+1}^T \bar{\mathbf{b}}$)	Liquid	Gas	Number of iterations
4	1.999d0	6.591d-4	21(21)
	7.221d-1	1.278d0	
40	1.999d0	6.591d-4	11(21)
	1.872d1	1.278d0	
400	1.999d2	6.591d-4	5(21)
	1.987d2	1.278d0	
4000	1.999d3	6.591d-4	2(21)
	1.999d3	1.278d0	

5.3 Scalability Results

In order to discuss the performance of the method, Table 4 illustrates the computational results obtained for various values of $n + 1$ (number of chemical species in the system), for a given choice of $\bar{\mathbf{b}}$. The tolerance for the stopping criterion of the interior-point method is 10^{-7} . We illustrate the number of iterations for the initialization procedure, the number of iterations of the interior-point method and the total CPU time. The number of iterations is increasing slightly but the general behavior of the algorithm remains the same. The increase of CPU time is only

due to the size increase of the linear systems. Figure 4 shows that the computational cost of the algorithm is proportional to the number $n + 1$ of chemical species involved, which makes its performance optimal.

Table 4: Sensitivity analysis of the resolution method with respect to the size of the system: number of iterations and CPU time.

$n + 1$	Size Linear Systems	# Iterations (init.)	# Iterations	CPU time
2	8	16	2	0.06
4	24	31	30	0.19
8	80	33	29	0.45
18	360	31	45	0.66
20*	440	31	46	0.81
30*	960	35	50	1.37

(\star systems with no chemical significance.)

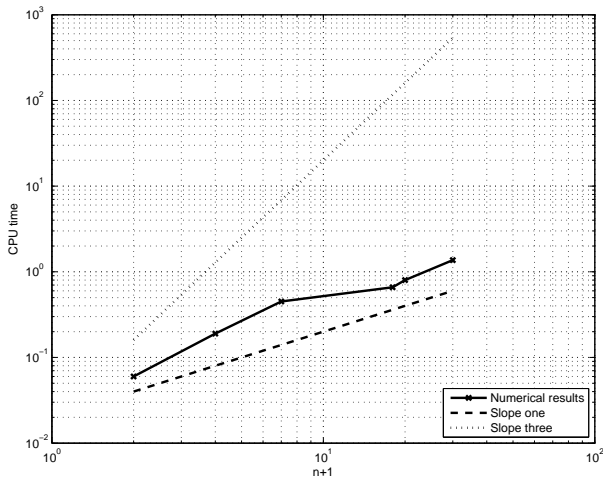


Figure 4: Scalability of the numerical method: Log-log plot of the CPU times for the interior-point method, vs. the number of chemical components $n + 1$; numerical results (solid line); line of slope one (dashed line); line of slope three corresponding to direct methods (pointed line).

5.4 Comparison with Existing NLP Solvers

In order to benchmark our solution method and the underlying linear algebra methods, a comparison of the proposed method with the NLP solver IPOPT [47, 43] is achieved. The nonlinear problem (1)-(5) is inserted in IPOPT, version 3.3.5. The unknowns for the IPOPT solver are condensed in the vector $X = (\mathbf{n}_g, \mathbf{x}_\alpha, y_\alpha)$ of size $n + 1 + (n + 1)P + P$, with $P = n + 1$. The initialization of the variables in IPOPT is done as follows. The values of \mathbf{n}_g is given by the the solution obtained by the present algorithm, *i.e.* supposedly the exact solution. The

mole fractions $\bar{\mathbf{z}}_\alpha^0$ are initialized in a neighborhood $\Delta_n \cap \mathcal{N}$ of the vertices of Δ_n where the function f is convex and $\nabla^2 f(\bar{\mathbf{z}}_\alpha^0) > 0$. The variables \bar{y}_α^0 are the barycentric coordinates of $(\mathbf{e}_{n+1}^T(\mathbf{b} - \mathbf{n}_g))^{-1}(\mathbf{b} - \mathcal{P}\mathbf{n}_g) \in \Delta_n$ in terms of $\bar{\mathbf{z}}_\alpha^0$. The variables \mathbf{x}_α^0 are given by $(\mathbf{z}_\alpha^0, 1 - \mathbf{e}_n^T \mathbf{z}_\alpha^0)$. The initialization of the variables in IPOPT corresponds exactly to the initialization of the same variables in the proposed algorithm, before the procedure presented in Section 4.

Default IPOPT options are used in the numerical experiments. The NLP problem is not scaled. The adaptive update strategy for the barrier parameter is used. The desired minimum relative distance from the initial point to bounds is set to 10^{-12} to take into account the various scales of the problem.

The three components system composed by 1-hexacosanol ($\text{C}_{26}\text{H}_{54}\text{O}$), pinic acid ($\text{C}_9\text{H}_{14}\text{O}_4$) and water (H_2O) at temperature 298.15 [K] and pressure 1 [atm] is considered again ($n+1 = 3$). It corresponds to a problem with 15 unknowns and 6 equality constraints. Results for the comparison of IPOPT with the present algorithm are given in Tables 5 and 6 for various examples that are representative of possible outcomes. These examples show that the proposed approach, which is adapted to the special nonlinear character of the thermodynamic equilibrium problem, can be more efficient than IPOPT in some cases.

The first and second examples show that the number of iterations can be much smaller with the new method (IPOPT does not converge in 10000 iterations in the second example, but provides a similar solution). The first example shows that IPOPT falls in a local minimum, for which one inequality constraint has been deactivated. The third example shows that it is possible for IPOPT to be trapped in a local minimum, by allowing the third phase to jump from one convex region to the other and be confounded with the first phase. The fourth example shows an example for which the determination of active constraints is difficult since one constraint is close to being deactivated. IPOPT finds a solution with a smaller objective function value in that case, although both minimizers (for IPOPT and the proposed method) are close to each other. The proposed method suffers here from the active sets strategy.

In summary, one can see the benefit of trying to take advantage of the information available *a priori* about such a strongly nonlinear problem, such as the information about the geometry of the objective function, or about the supporting tangent plane. In particular, the proposed algorithm provides a natural justification to the treatment of linearly dependent constraints due to dependent phases: numerical results show that the combination of active sets and interior-point methods allow to handle appropriately the merging of dependent phases in most cases. These results are consistent with those presented in [2], that already exhibited an accurate selection of phases.

Conclusion

An interior-point method for the determination of the thermodynamic equilibrium of gas-liquid atmospheric particles has been presented. It relies on a perturbation of the problem of determining the convex hull of the energy function for liquid phases. A least-squares technique for the initialization of the interior-point method allows to start the algorithm in a neighborhood of the global optimum, and favor convergence toward this optimum. Sequential quadratic programming techniques allow to decouple the various scales of the physical problem and solve efficiently the KKT Newton system. Numerical results have shown the efficiency of the method

Table 5: Comparison with NLP solver IPOPT [47]. Examples for (1) $\bar{\mathbf{b}} = (1.0716d0, 1.3025d0, 3.5424d0)^T$ and (2) $\bar{\mathbf{b}} = (2.0721d0, 2.3029d0, 9.8165d0)^T$,

		\mathbf{n}_g	\mathbf{x}_1	\mathbf{x}_2	\mathbf{x}_3	y_α	# iter.	Objective fct
(1)	Algorithm Proposed	4.8548d-4	6.0900d-1	2.3294d-3	3.4011d-12	1.7494d0	44	-1.6454d0
		3.6365d-4	2.1894d-1	3.7159d-1	3.3508d-3	2.4697d0		
		1.2740d0	1.7204d-1	6.2607d-1	9.9664d-1	4.2255d-1		
IPOPT		4.9272d-4	6.1972d-1	1.3621d-3	7.7221d-1	1.7221d0	231	-1.5908d0
		3.4130d-4	2.0582d-1	3.2987d-1	1.8479d-1	2.8730d0		
		1.3206d0	1.7444d-1	6.6876d-1	4.2984d-2	0d0		
(2)	Algorithm Proposed	4.9428d-4	3.2918d-12	3.2918d-12	6.2688d-1	8.1545d0	44	-4.2747d0
		3.4507d-4	3.1347d-3	3.1347d-3	2.0627d-1	1.d-8		
		1.2742d0	9.9686d-1	9.9686d-1	1.6683d-1	9.5702d0		
IPOPT		5.0945d-4	1.4912d-7	5.6051d-1	5.4194d-1	6.6926d0	10000	-4.2746d0
		3.6078d-4	3.7114d-3	1.8949d-1	1.7839d-1	8.1397d-4		
		1.2742d0	9.9628d-1	2.4998d-1	2.7966d-1	11.0313d0		

Table 6: Comparison with NLP solver IPOPT [47]. Examples for (3) $\bar{\mathbf{b}} = (6.d0, 2.d0, 11.d0)^T$, and (4) $\bar{\mathbf{b}} = (1.d0, 10.d0, 10.d0)^T$.

		\mathbf{n}_g	\mathbf{x}_1	\mathbf{x}_2	\mathbf{x}_3	y_α	# iter.	Objective fct
(3)	Algorithm Proposed	4.8548d-4	6.0900d-1	2.3294d-3	3.4011d-12	3.3858d0	38	-2.9905d0
		3.6365d-4	2.1894d-1	3.7159d-1	3.3507d-3	4.1529d0		
		1.2740d0	1.7204d-1	6.2608d-1	9.9664d-1	5.3778d0		
IPOPT		5.0908d-4	6.3567d-1	4.5373d-5	6.3567d-1	1.6291d0	5527	-2.5390d0
		3.1693d-4	1.8809d-1	1.7683d-1	1.8809d-1	9.5556d0		
		1.3768d0	1.7622d-1	8.2312d-1	1.7622d-1	1.6291d0		
(4)	Algorithm Proposed	8.3906d-4	9.3406d-3	5.0223d-2	5.0223d-1	2.1d-7	261	-8.8152d0
		4.3410d-4	4.598d-1	5.0263d-1	5.0263d-1	1.9894d1		
		1.1044d0	5.3077d-1	4.4714d-1	4.4714d-1	1d-8		
IPOPT		4.6326d-4	5.6915d-1	8.8745d-3	1.0931d-1	1.4677d0	448	-9.2931d0
		4.6990d-4	2.7800d-1	5.1855d-1	5.7381d-1	1.8496d1		
		1.0347d0	1.5283d-1	4.7257d-1	3.1686d-1	0.d0		

for the computation of the thermodynamic partitioning of chemical species between gas phase and liquid phases, and its importance compared to pure liquid equilibrium calculations. Com-

parisons with the NLP solver IPOPT have shown that the proposed approach is competitive for this application.

Acknowledgments

The author wishes to thank Professor Jiwen He, Department of Mathematics, University of Houston, for fruitful remarks and discussions, and the anonymous referees for their valuable comments to improve the manuscript.

A Proof of Theorem 4

Theorem *In a neighborhood of a KKT point, the displacements $\mathbf{p}_{\mathbf{z}_\alpha}$, $\alpha = 1, \dots, P$ and $\mathbf{p}_{\mathbf{y}} = (\mathbf{p}_{y_\alpha})_{\alpha=1}^P$ in (19) are linear functions of \mathbf{p}_g , i.e.*

$$\begin{aligned}\mathbf{p}_{\mathbf{y}} &= \tilde{\mathbf{A}}_{\mathbf{y}}\mathbf{p}_g + \tilde{\mathbf{B}}_{\mathbf{y}} \\ \mathbf{p}_{\mathbf{z}_\alpha} &= \tilde{\mathbf{A}}_{\mathbf{z}_\alpha}\mathbf{p}_g + \tilde{\mathbf{B}}_{\mathbf{z}_\alpha}, \quad \alpha = 1, \dots, P.\end{aligned}$$

Proof. The explicit expression of the increments is obtained by the combination of range-space and null-space methods. Under assumption (H5), the direction $\mathbf{p}_{\mathbf{z}_\alpha}$ is first eliminated from the system (13). It follows that

$$\mathbf{p}_{\mathbf{z}_\alpha} = y_\alpha^{-1}\mathbf{H}_\alpha^{-1}(\mathbf{b}_{\mathbf{z}_\alpha} - (\nabla f + \boldsymbol{\eta})p_{y_\alpha} - y_\alpha\mathbf{p}_\boldsymbol{\eta} + y_\alpha\mathbf{T}_\boldsymbol{\eta}\mathbf{p}_g), \quad (26)$$

The resulting Schur complement system is

$$\begin{aligned}\mathbf{S}_\boldsymbol{\eta}\mathbf{p}_\boldsymbol{\eta} + \sum_{\alpha=1}^P \mathbf{v}_\alpha p_{y_\alpha} &= \mathbf{d}_\boldsymbol{\eta}, \\ \mathbf{v}_\alpha^T \mathbf{p}_\boldsymbol{\eta} - (\mathbf{e}_{n+1}^T \mathbf{x}_\alpha)p_\gamma - y_\alpha^{-1}(\theta_\alpha - w_\alpha)p_{y_\alpha} &= d_{y_\alpha}, \alpha = 1, \dots, P, \\ \sum_{\alpha=1}^P (\mathbf{e}_{n+1}^T \mathbf{x}_\alpha)p_{y_\alpha} &= b_\gamma - \mathbf{T}_\gamma \mathbf{p}_g,\end{aligned} \quad (27)$$

where

$$\begin{aligned}\mathbf{S}_\boldsymbol{\eta} &= \sum_{\alpha=1}^P y_\alpha \mathbf{H}_\alpha^{-1}, & \mathbf{v}_\alpha &= \mathbf{H}_\alpha^{-1}(\nabla f + \boldsymbol{\eta}) - \mathbf{z}_\alpha, \\ w_\alpha &= (\nabla f + \boldsymbol{\eta})^T \mathbf{H}_\alpha^{-1}(\nabla_{\mathbf{z}_\alpha} f + \boldsymbol{\eta}), & \mathbf{d}_\boldsymbol{\eta} &= \mathbf{b}_H - \mathbf{b}_\boldsymbol{\eta} + \mathbf{T}_\boldsymbol{\eta} \mathbf{p}_g, \\ d_{y_\alpha} &= y_\alpha^{-1}(\nabla f + \boldsymbol{\eta})^T \mathbf{H}_\alpha^{-1} \mathbf{b}_{\mathbf{z}_\alpha} - b_{y_\alpha}, & \mathbf{b}_H &= \sum_{\alpha=1}^P \mathbf{H}_\alpha^{-1} \mathbf{b}_{\mathbf{z}_\alpha},\end{aligned}$$

Under assumption (H5) again, the Schur complement $\mathbf{S}_\boldsymbol{\eta}$ is positive definite and the direction $\mathbf{p}_\boldsymbol{\eta}$ is now eliminated from (27) by solving for $\mathbf{S}_\boldsymbol{\eta}$:

$$\mathbf{p}_\boldsymbol{\eta} = \mathbf{S}_\boldsymbol{\eta}^{-1} \left(\mathbf{d}_\boldsymbol{\eta} - \sum_{\alpha=1}^P \mathbf{v}_\alpha p_{y_\alpha} \right). \quad (28)$$

This elimination gives the resulting system:

$$\begin{aligned}\mathbf{S}_y \mathbf{p}_y + \mathbf{u} p_\gamma &= \mathbf{h}_y, \\ \mathbf{u}^T \mathbf{p}_y &= b_\gamma - \mathbf{T}_\gamma \mathbf{p}_g,\end{aligned}\tag{29}$$

where

$$\begin{aligned}\mathbf{S}_y &= \mathbf{V}^T \mathbf{S}_\eta^{-1} \mathbf{V} + \text{diag}(y_\alpha^{-1}(\theta_\alpha - w_\alpha)) \quad \text{with } \mathbf{V} = (\mathbf{v}_\alpha) \in \mathbb{R}^{n \times P}, \\ \mathbf{u} &= \mathbf{X}^T \mathbf{e}_n \quad \text{with } \mathbf{X} = (\mathbf{x}_\alpha) \in \mathbb{R}^{n \times P}, \\ \mathbf{h}_y &= (h_{y_\alpha}) \in \mathbb{R}^P \quad \text{with } h_{y_\alpha} = \mathbf{v}_\alpha^T \mathbf{S}_\eta^{-1} \mathbf{d}_\eta - d_{y_\alpha} \\ \mathbf{p}_y &= (p_{y_\alpha}) \in \mathbb{R}^P.\end{aligned}$$

We distinguish from now on the cases $P > 1$ and $P = 1$. When $P > 1$, assumption (H3) (affine independence) implies that \mathbf{Z} is of full column rank if $P < n + 1$, which implies that \mathbf{S}_y is positive definite. However, the Schur complement \mathbf{S}_y is singular when the number of phases P is equal to the number of components $n + 1$, since \mathbf{V} is not of full column rank. Therefore, a direct inversion of \mathbf{S}_y is intractable. A null-space method is therefore applied in a neighborhood of a KKT point to express \mathbf{p}_y as $\mathbf{p}_y = \mathbf{p}_y^0 + \mathbf{Z}_u \mathbf{p}_{\bar{y}}$, where $\mathbf{Z}_u = \begin{pmatrix} \mathbf{I}_{P-1} \\ -\frac{1}{\mathbf{u}_P} \mathbf{u}_{1:P-1}^T \end{pmatrix} \in \mathbb{R}^{P \times (P-1)}$ is the null-space matrix such that $\mathbf{Z}_u^T \mathbf{u} = \mathbf{0}$ and $\mathbf{p}_y^0 = (\mathbf{0}, \frac{1}{\mathbf{u}_P} (b_\gamma - \mathbf{T}_\gamma \mathbf{p}_g))^T$ is a particular solution in the null-space. Then $\mathbf{p}_{\bar{y}}$ is obtained by solving the reduced system

$$\mathbf{Z}_u^T \mathbf{S}_y \mathbf{Z}_u \mathbf{p}_{\bar{y}} = \mathbf{Z}_u^T \mathbf{h}_y - \mathbf{Z}_u^T \mathbf{S}_y \mathbf{p}_y^0.\tag{30}$$

In a neighborhood of a KKT point, the following relations hold:

$$\mathbf{Z}_u \simeq \mathbf{Z}_{e_P},\tag{31a}$$

$$\mathbf{Z}_u^T \mathbf{S}_y \mathbf{Z}_u \simeq \mathbf{Z}_{e_P}^T \mathbf{Z}^T \mathbf{S}_\eta^{-1} \mathbf{Z} \mathbf{Z}_{e_P} + \mathbf{Z}_{e_P}^T \text{diag}(y_\alpha^{-1} \theta_\alpha) \mathbf{Z}_{e_P},\tag{31b}$$

$$(\nabla f + \boldsymbol{\eta}) \simeq \mathbf{0},\tag{31c}$$

$$\mathbf{V} \simeq -\mathbf{Z},\tag{31d}$$

and the Schur complement \mathbf{S}_y is approximately equal to $\mathbf{S}_y \approx \mathbf{Z}^T \mathbf{S}_\eta^{-1} \mathbf{Z} + \text{diag}(y_\alpha^{-1} \theta_\alpha)$. Assumption (H3) implies that $\mathbf{Z} = (\mathbf{z}_\alpha) \in \mathbb{R}^{n \times P}$ is of full column rank if $P < n$, which implies that \mathbf{S}_y is positive definite. But, the Schur complement \mathbf{S}_y is singular if $P = n$. Therefore, the range space method cannot be used for the solution to (29) and hence a null-space method is used. Assumption (H6) implies that $\mathbf{Z} \mathbf{Z}_{e_P} = (\mathbf{z}_1 - \mathbf{z}_P, \dots, \mathbf{z}_{P-1} - \mathbf{z}_P)$ is of full column rank and the reduced Schur complement is positive definite. Let us define the auxiliary matrix:

$$\mathbf{T}_y = \mathbf{Z}_u (\mathbf{Z}_u^T \mathbf{S}_y \mathbf{Z}_u)^{-1} \mathbf{Z}_u^T.\tag{32}$$

By using (32) and (31a-d), (30) gives:

$$\begin{aligned}
\mathbf{p}_y &= (\mathbf{I} - \mathbf{T}_y \mathbf{S}_y) \begin{pmatrix} 0 \\ \frac{1}{\mathbf{u}_P} \end{pmatrix} (b_\gamma - \mathbf{T}_\gamma \mathbf{p}_g) + (\mathbf{T}_y \mathbf{Z}^T \mathbf{S}_\eta^{-1}) (\mathbf{b}_\eta - \mathbf{T}_\eta \mathbf{p}_g) \\
&\quad - \mathbf{T}_y \left(\mathbf{Z}^T \mathbf{S}_\eta^{-1} \sum_\alpha \mathbf{H}_\alpha^{-1} \mathbf{b}_{z_\alpha} - \mathbf{b}_y \right)
\end{aligned} \tag{33}$$

Relation (20) is obtained by setting

$$\tilde{\mathbf{A}}_y = -(\mathbf{I} - \mathbf{T}_y \mathbf{S}_y) \begin{pmatrix} \mathbf{0} \\ (\mathbf{x}_P^T \mathbf{e}_{n+1})^{-1} \end{pmatrix} \mathbf{T}_\gamma - (\mathbf{T}_y \mathbf{Z}^T \mathbf{S}_\eta^{-1}) \mathbf{T}_\eta$$

and

$$\tilde{\mathbf{B}}_y = \tilde{\mathbf{d}}_y + (\mathbf{I} - \mathbf{T}_y \mathbf{S}_y) \begin{pmatrix} \mathbf{0} \\ (\mathbf{x}_P^T \mathbf{e}_{n+1})^{-1} \end{pmatrix} b_\gamma + \mathbf{T}_y \mathbf{Z}^T \mathbf{S}_\eta^{-1} \mathbf{b}_\eta,$$

where $\tilde{\mathbf{d}}_y = \mathbf{T}_y \mathbf{b}_y - \mathbf{T}_y \mathbf{Z}^T \mathbf{S}_\eta^{-1} \mathbf{b}_H$. The increment p_γ is obtained with

$$p_\gamma = \mathbf{u}^{-1} (\mathbf{h}_y - \mathbf{S}_y \mathbf{p}_y),$$

where \mathbf{u}^{-1} is a left-inverse of \mathbf{u} . Then (21) is obtained starting from (26). First (31a-d) allow to write:

$$\begin{aligned}
\mathbf{p}_{z_\alpha} &= y_\alpha^{-1} \mathbf{H}_\alpha^{-1} \mathbf{b}_{z_\alpha} - \mathbf{H}_\alpha^{-1} \mathbf{S}_\eta^{-1} \mathbf{d}_\eta + \mathbf{H}_\alpha^{-1} \mathbf{S}_\eta^{-1} \mathbf{V}^T \mathbf{p}_y + \mathbf{H}_\alpha^{-1} \mathbf{T}_\eta \mathbf{p}_g \\
&= y_\alpha^{-1} \mathbf{H}_\alpha^{-1} \mathbf{b}_{z_\alpha} - \mathbf{H}_\alpha^{-1} \mathbf{S}_\eta^{-1} (\mathbf{b}_H - \mathbf{b}_\eta + \mathbf{T}_\eta \mathbf{p}_g) - \mathbf{H}_\alpha^{-1} \mathbf{S}_\eta^{-1} \mathbf{Z}^T \mathbf{p}_y + \mathbf{H}_\alpha^{-1} \mathbf{T}_\eta \mathbf{p}_g
\end{aligned} \tag{34}$$

Plugging (33) into (34) gives

$$\begin{aligned}
\mathbf{p}_{z_\alpha} &= y_\alpha^{-1} \mathbf{H}_\alpha^{-1} \mathbf{b}_{z_\alpha} - \mathbf{H}_\alpha^{-1} \mathbf{S}_\eta^{-1} (\mathbf{b}_H - \mathbf{b}_\eta + \mathbf{T}_\eta \mathbf{p}_g) \\
&\quad - \mathbf{H}_\alpha^{-1} \mathbf{S}_\eta^{-1} \mathbf{Z}^T (\mathbf{I} - \mathbf{T}_y \mathbf{S}_y) \begin{pmatrix} \mathbf{0} \\ (\mathbf{x}_P^T \mathbf{e}_{n+1})^{-1} \end{pmatrix} (b_\gamma - \mathbf{T}_\gamma \mathbf{p}_g) \\
&\quad - \mathbf{H}_\alpha^{-1} \mathbf{S}_\eta^{-1} \mathbf{Z}^T (\mathbf{T}_y \mathbf{Z} \mathbf{S}_\eta^{-1}) (\mathbf{b}_\eta - \mathbf{T}_\eta \mathbf{p}_g) \\
&\quad + \mathbf{H}_\alpha^{-1} \mathbf{S}_\eta^{-1} \mathbf{Z}^T \mathbf{T}_y \mathbf{Z} \mathbf{S}_\eta^{-1} \mathbf{b}_H - \mathbf{H}_\alpha^{-1} \mathbf{S}_\eta^{-1} \mathbf{Z}^T \mathbf{T}_y \mathbf{b}_y + \mathbf{H}_\alpha^{-1} \mathbf{T}_\eta \mathbf{p}_g
\end{aligned} \tag{35}$$

Conclusion for $P > 1$ is straightforward by re-arranging the terms and setting

$$\tilde{\mathbf{A}}_{z_\alpha} = \mathbf{H}_\alpha^{-1} \left[(-\mathbf{S}_\eta^{-1} + \mathbf{S}_\eta^{-1} \mathbf{Z}^T \mathbf{T}_y \mathbf{Z} \mathbf{S}_\eta^{-1}) \mathbf{T}_\eta + \mathbf{S}_\eta^{-1} \mathbf{Z}^T (\mathbf{I} - \mathbf{T}_y \mathbf{S}_y) \begin{pmatrix} \mathbf{0} \\ (\mathbf{x}_P^T \mathbf{e}_{n+1})^{-1} \end{pmatrix} \mathbf{T}_\gamma + \mathbf{T}_\eta \right]$$

and

$$\begin{aligned}
\tilde{\mathbf{B}}_{z_\alpha} &= y_\alpha^{-1} \mathbf{H}_\alpha^{-1} \mathbf{b}_{z_\alpha} \\
&\quad - \mathbf{H}_\alpha^{-1} \left[\tilde{\mathbf{d}}_z - (\mathbf{S}_\eta^{-1} + \mathbf{S}_\eta^{-1} \mathbf{Z}^T \mathbf{T}_y \mathbf{Z} \mathbf{S}_\eta^{-1}) \mathbf{b}_\eta + \mathbf{S}_\eta^{-1} \mathbf{Z}^T (\mathbf{I} - \mathbf{T}_y \mathbf{S}_y) \begin{pmatrix} \mathbf{0} \\ (\mathbf{x}_P^T \mathbf{e}_{n+1})^{-1} \end{pmatrix} b_\gamma \right]
\end{aligned}$$

for $\alpha = 1, \dots, P$ and $\tilde{\mathbf{d}}_{\mathbf{z}} = \mathbf{S}_{\eta}^{-1}\mathbf{b}_H - \mathbf{S}_{\eta}^{-1}\mathbf{Z}^T\mathbf{T}_y\mathbf{Z}\mathbf{S}_{\eta}^{-1}\mathbf{b}_H + \mathbf{S}_{\eta}^{-1}\mathbf{Z}\mathbf{T}_y\mathbf{b}_y$. Conclusion for $P > 1$ follows.

For the case $P = 1$, the demonstration is based on similar steps. We denote $\mathbf{p}_y = (\mathbf{p}_{yP})$. The increments \mathbf{p}_y and p_{γ} are the straightforward solutions of

$$\begin{aligned}\mathbf{S}_y\mathbf{p}_y + \mathbf{u}p_{\gamma} &= \mathbf{h}_y \\ \mathbf{u}^T\mathbf{p}_y &= b_{\gamma} - \mathbf{T}_{\gamma}\mathbf{p}_g.\end{aligned}$$

and we obtain:

$$\mathbf{p}_y = \frac{1}{\mathbf{u}_P} (b_{\gamma} - \mathbf{T}_{\gamma}\mathbf{p}_g). \quad (36)$$

Relationship (21) is obtained by setting $\tilde{\mathbf{A}}_y = -\frac{1}{\mathbf{x}_P^T\mathbf{e}_{n+1}}\mathbf{T}_{\gamma}$ and $\tilde{\mathbf{B}}_y = \frac{b_{\gamma}}{\mathbf{x}_P^T\mathbf{e}_{n+1}}$.

In a neighborhood of a KKT point, relationships (26), (28) and (36) lead to

$$\mathbf{p}_{\mathbf{z}_{\alpha}} = y_{\alpha}^{-1}\mathbf{H}_{\alpha}^{-1}\mathbf{b}_{\mathbf{z}_{\alpha}} - \mathbf{H}_{\alpha}^{-1}\mathbf{S}_{\eta}^{-1}(\mathbf{b}_H - \mathbf{b}_{\eta} + \mathbf{T}_{\eta}\mathbf{p}_g) - \mathbf{H}_{\alpha}^{-1}\mathbf{S}_{\eta}^{-1}\mathbf{Z}^T\frac{1}{\mathbf{u}_P}(b_{\gamma} - \mathbf{T}_{\gamma}\mathbf{p}_g) + \mathbf{H}_{\alpha}^{-1}\mathbf{T}_{\eta}\mathbf{p}_g$$

and conclusion follows by setting $\tilde{\mathbf{A}}_{\mathbf{z}_{\alpha}} = \mathbf{H}_{\alpha}^{-1}\left[\mathbf{S}_{\eta}^{-1}\left(-\mathbf{T}_{\eta} + \mathbf{Z}^T\frac{1}{\mathbf{x}_P^T\mathbf{e}_{n+1}}\mathbf{T}_{\gamma}\right) + \mathbf{T}_{\eta}\right]$ and $\tilde{\mathbf{B}}_{\mathbf{z}_{\alpha}} = y_{\alpha}^{-1}\mathbf{H}_{\alpha}^{-1}\mathbf{b}_{\mathbf{z}_{\alpha}} - \mathbf{H}_{\alpha}^{-1}\left[\mathbf{S}_{\eta}^{-1}\left(\mathbf{b}_H - \mathbf{b}_{\eta} + \mathbf{Z}^T\frac{1}{\mathbf{x}_P^T\mathbf{e}_{n+1}}b_{\gamma}\right)\right]$, $\alpha = P = 1$. ■

References

- [1] N. Amundson, A. Caboussat, J. W. He, and J. H. Seinfeld. An optimization problem related to the modeling of atmospheric organic aerosols. *C. R. Acad. Sci. Paris, Série I*, 340(10):765–768, 2005.
- [2] N. R. Amundson, A. Caboussat, J. W. He, and J. H. Seinfeld. Primal-dual interior-point algorithm for chemical equilibrium problems related to modeling of atmospheric organic aerosols. *J. Optim. Theory Appl.*, 130(3):375–407, 2006.
- [3] N. R. Amundson, A. Caboussat, J. W. He, J. H. Seinfeld, and K. Y. Yoo. A primal-dual active-set algorithm for chemical equilibrium problems related to modeling of atmospheric inorganic aerosols. *J. Optim. Theory Appl.*, 128(3):469–498, 2006.
- [4] N.R. Amundson, A. Caboussat, C. Landry, J. W. He, and J. H. Seinfeld. A dynamic optimization problem related to organic aerosols. *C. R. Acad. Sci. Paris, Série I*, 344(8):519–522, 2007.
- [5] J. Benoist and J.-B. Hiriart-Urruty. What is the subdifferential of the closed convex hull of a function? *SIAM J. Numer. Anal.*, 27(6), 1996.

- [6] H. Y. Benson, A. Sen, D. F. Shanno, and R. J. Vanderbei. Interior-point algorithms, penalty methods and equilibrium problems. *Computational Optimization and Applications*, 34(3):155–182, 2006.
- [7] H. Y. Benson and D. F. Shanno. Interior-point methods for nonconvex nonlinear programming: regularization and warmstarts. *Computational Optimization and Applications*, 40(2):143–189, 2007.
- [8] H. Y. Benson, D. F. Shanno, and R. J. Vanderbei. Interior-point methods for nonconvex nonlinear programming: Jamming and numerical testing. *Math. Program.*, 99(1):35–48, 2004.
- [9] R. Byrd, J. Ch. Gilbert, and J. Nocedal. A trust region method based on interior point techniques for nonlinear programming. *Math. Program.*, 89:149–185, 2000.
- [10] R. Byrd, M. E. Hribar, and J. Nocedal. An interior point method for large scale nonlinear programming. *SIAM J. Optimization*, 9(4):877–900, 1999.
- [11] R. H. Byrd, J. Nocedal, and R. A. Waltz. KNITRO: An integrated package for nonlinear optimization. In G. di Pillo and M. Roma, editors, *Large-Scale Nonlinear Optimization*, pages 35–59. Springer-Verlag, 2006.
- [12] N. Cohen and J. Dancis. Inertias of block band matrix completions. *SIAM J. Matrix Analysis and Applications*, 19(3):583–612, 1998.
- [13] K. Denbigh. *The Principles of Chemical Equilibrium*. Cambridge University Press, third edition, 1971.
- [14] A. El-Bakry, R. Tapia, T. Tsuchiya, and Y. Zhang. On the formulation and theory of the Newton interior-point method for nonlinear programming. *J. Optim. Theory Appl.*, 89(3):507–541, 1996.
- [15] F. Facchinei, A. Fischer, and C. Kanzow. On the accurate identification of active constraints. *SIAM J. Optim.*, 9(1):14–32, 1998.
- [16] A. V. Fiacco and G. P. McCormick. *Nonlinear Programming: Sequential Unconstrained Minimization Techniques*. John Wiley and Sons, Inc, 1968.
- [17] A. Forsgren and P. E. Gill. Primal-dual interior methods for nonconvex nonlinear programming. *SIAM Journal on Optimization*, 8:1132–1152, 1998.
- [18] A. Forsgren, P. E. Gill, and M. H. Wright. Interior methods for nonlinear optimization. *SIAM Review*, 44(4):525–597, 2002.
- [19] A. Fredenslund, J. Gmehling, and P. Rasmussen. *Vapor-Liquid Equilibrium Using UNIFAC*. Elsevier, Amsterdam, Netherlands, 1977.
- [20] P. E. Gill, W. Murray, M. A. Saunders, and M. H. Wright. Inertia-controlling methods for general quadratic programming. *SIAM Review*, 33(1):1–36, 1991.

- [21] J. Gondzio and A. Grothey. Direct solution of linear systems of size 10^9 arising in optimization with interior point methods. In *Lecture Notes in Computer Science*, pages 513–525. Springer-Verlag, Berlin, 2006.
- [22] Y. Jiang, G. R. Chapman, and W. R. Smith. On the geometry of chemical reaction and phase equilibria. *Fluid Phase Equilibria*, 118(1):77–102, 1996.
- [23] Y. P. Kim and J. H. Seinfeld. Atmospheric gas-aerosol equilibrium III: Thermodynamics of crustal elements Ca^{2+} , K^+ , and Mg^{2+} . *Aerosol Science and Technology*, 22:93–110, 1995.
- [24] D. A. Kulik. A Gibbs energy minimization approach to model sorption equilibria at the mineral-water interface: Thermodynamic relations for multi-site-surface complexation. *Amer. J. Sci.*, 302:227–279, 2002.
- [25] A. Lucia, L. Padmanabhan, and S. Venkataraman. Multiphase equilibrium flash calculations. *Computers and Chemical Engineering*, 24(12):2557 – 2569, 2000.
- [26] C. M. McDonald and C. A. Floudas. Global optimization and analysis for the Gibbs free energy function for the UNIFAC, Wilson, and ASOG equations. *Industrial and Engineering Chemistry Research*, 34:1674–1687, 1995.
- [27] C. M. McDonald and C. A. Floudas. GLOPEQ: A new computational tool for the phase and chemical equilibrium problem. *Computers and Chemical Engineering*, 21(1):1–23, 1996.
- [28] K. McKinnon, C. Millar, and M. Mongeau. Global optimization for the chemical and phase equilibrium problem using interval analysis. In *State of the art in global optimization*, pages 365–381. Kluwer Acad. Publ., 1996.
- [29] K. McKinnon and M. Mongeau. A generic global optimization algorithm for the chemical and phase equilibrium problem. *J. Global Optim.*, 12(4):325–351, 1998.
- [30] M. L. Michelsen. The isothermal flash problem. Part I: Stability. *Fluid Phase Equilibria*, 9(1):1–19, 1982.
- [31] A. Nenes, S. N. Pandis, and C. Pilinis. ISORROPIA: A new thermodynamic equilibrium model for multiphase multicomponent inorganic aerosols. *Aquatic Geochemistry*, 4:123–152, 1998.
- [32] J. Nocedal and S. J. Wright. *Numerical Optimization*. Springer-Verlag, 1999.
- [33] J. F. Pankow. An absorption model of gas/particle partitioning of organic compounds in the atmosphere. *Atmos. Env.*, 28(2):185–188, 1994.
- [34] J. F. Pankow. An absorption model of the gas/aerosol partitioning involved in the formation of secondary organic aerosol. *Atmos. Env.*, 28(2):189–193, 1994.
- [35] B. E. Poling, J. M. Prausnitz, and J. P. Connell. *Properties of Gases and Liquids*. McGraw-Hill, 2001.

- [36] P. J. Rabier and A. Griewank. Generic aspects of convexification with applications to thermodynamic equilibrium. *Archive for Rational Mechanics and Analysis*, 118(4):349–397, 1992.
- [37] R. T. Rockafellar. *Convex Analysis*. Princeton University Press, Reprint edition, 1996.
- [38] J. H. Seinfeld and S. N. Pandis. *Atmospheric Chemistry and Physics: From Air Pollution to Climate Change*. Wiley, New York, 1998.
- [39] J. V. Smith, R. W. Missen, and W. R. Smith. General optimality criteria for multiphase multireaction chemical equilibrium. *AIChE Journal*, 39(4):707–710, 1993.
- [40] Y. S. Teh and G. P. Rangaiah. Tabu search for global optimization of continuous functions with application to phase equilibrium calculations. *Computers and Chemical Engineering*, 27(11):1665–1679, 2003.
- [41] A. L. Tits, A. Wachter, S. Bakhtiari, T. J. Urban, and C. T. Lawrence. A primal-dual interior-point method for nonlinear programming with strong global and local convergence properties. *SIAM Journal on Optimization*, 14(1):173–199, 2003.
- [42] R. J. Vanderbei. LOQO: An interior point code for quadratic programming. *Optimization Methods and Software*, 11(1–4):451–484, 1999.
- [43] A. Wächter. *An Interior Point Algorithm for Large-Scale Nonlinear Optimization with Applications in Process Engineering*. PhD thesis, Carnegie Mellon University, 2002.
- [44] A. Wächter and L. T. Biegler. Failure of global convergence for a class of interior point methods for nonlinear programming. *Mathematical Programming*, 88(3):565–574, 2000.
- [45] A. Wächter and L. T. Biegler. Line search filter methods for nonlinear programming: Local convergence. *SIAM Journal on Optimization*, 16(1):32–48, 2005.
- [46] A. Wächter and L. T. Biegler. Line search filter methods for nonlinear programming: Motivation and global convergence. *SIAM Journal on Optimization*, 16(1):1–31, 2005.
- [47] A. Wächter and L. T. Biegler. On the implementation of a primal-dual interior point filter line search algorithm for large-scale nonlinear programming. *Mathematical Programming*, 106(1):25–57, 2006.
- [48] S. K. Wasylkiewicz, L. N. Sridhar, M. F. Doherty, and M. F. Malone. Global stability analysis and calculation of liquid-liquid equilibrium in multicomponent mixtures. *Industrial and Engineering Chemistry Research*, 35:1395–1408, 1996.
- [49] H. Yamashita, H. Yabe, and T. Tanabe. A globally and superlinearly convergent primal-dual interior point trust region method for large scale constrained optimization. *Math. Program., Ser. A*, 102:111–151, 2005.